

NASA Technical Memorandum 81949

NASA-TM-81949 19810013531

Description of 0.186-Scale Model of High-Speed Duct of National Transonic Facility

Garl L. Gentry, Jr., William B. Igoe,
and Dennis E. Fuller

MAY 1981

LIBRARY COPY
MAY 14 1981
LANGLEY RESEARCH CENTER
LIBRARY, NASA
HAMPTON, VIRGINIA

NASA



NASA Technical Memorandum 81949

Description of 0.186-Scale
Model of High-Speed Duct
of National Transonic Facility

Garl L. Gentry, Jr., William B. Igoe,
and Dennis E. Fuller
*Langley Research Center
Hampton, Virginia*



National Aeronautics
and Space Administration

**Scientific and Technical
Information Branch**

1981

SUMMARY

The National Transonic Facility (NTF) is a pressurized cryogenic wind tunnel with a 2.5 m square test section. A 0.186-scale model of the NTF has been used to simulate the aerodynamic performance of the components of the high-speed duct of the NTF. These components consist of a wide-angle diffuser, settling chamber, contraction section, test section, model support section, and high-speed diffuser. The geometry of the model tunnel, referred to as the diffuser flow apparatus (DFA) is described, and some of its operating characteristics are presented.

The DFA is a wind tunnel with a 46.38 cm square test section which is operated at ambient temperature and pressure with air as the test gas. The DFA Mach number range, from about 0.1 to 1.2, duplicates that of the NTF. It has been used primarily to obtain an experimental assessment of the fan pressure ratio and power requirements for the NTF. It has also provided verification for the aerodynamic design of such components as the wide-angle diffuser, the contraction section, and the high-speed diffuser. Its capabilities also permit test-section slot shaping and flow generation studies.

INTRODUCTION

The need for high Reynolds number test capability at transonic speeds has been widely recognized. (See, for example, refs. 1 to 6.) However, it was not until the cryogenic approach was adopted, as proposed by Goodyer and Kilgore (ref. 7), that the desired test capability finally became attainable within the limitations of cost and acceptable model loads. The Goodyer and Kilgore proposal follows an earlier concept of using reduced temperature to increase Reynolds number initially suggested by Margoulis (ref. 8) and later advanced for cryogenic application by Smelt (ref. 9). In the United States, this concept has evolved into what is known as the National Transonic Facility (NTF), a 2.5-m transonic wind tunnel located at the NASA Langley Research Center in Hampton, Virginia. (See refs. 10 to 18.) In Europe, as a joint initiative, the AGARD countries of Great Britain, France, Germany, and The Netherlands have proposed a similar wind tunnel designated the European Transonic Windtunnel (ref. 19).

During the design of the NTF, a variety of wind-tunnel models were used to evaluate critical aspects of the NTF circuit. Among these models is a 0.186-scale replica of the high-speed duct of the new facility. This model, referred to as the diffuser flow apparatus (DFA), consists of a wide-angle diffuser, settling chamber, contraction section, test section, model support section, and high-speed diffuser. It was constructed on the site of an injector-driven hypersonic wind tunnel (ref. 20) and utilized the same compressors and ducting. The subsequent sections of this report describe the configuration and instrumentation for the major components of the DFA and present some of its measured flow characteristics.

The DFA has been used primarily to obtain an experimental assessment of the fan pressure ratio and power requirements for the NTF. Coincidentally, it has provided verification test capability for the design of such components as the wide-angle diffuser, the contraction section, and the high-speed diffuser. In addition, since the tunnel was designed to permit changes of various components, it has been useful for development testing for such components as the test section and the model support section.

With the use of extensive pressure tapping and some occasional strain-gage bridges, loads information has been obtained on the test-section beams, the reentry flaps, the model support strut, and on the walls of the model support section. Special test configurations permitted the investigation of diffuser spoiler flaps and a tunnel modification to allow high angle-of-attack settings of the model support strut. Unsteady measurements consisted of turbulence and noise investigations and of controls response tests (ref. 21) using impulsive and periodic excitation. A solid-wall configuration for the test section was used to investigate the aerodynamic characteristics of some candidate heat exchanger tube bundle configurations for the NTF. The test-section assembly has also been made so as to permit slot shaping and flow generation studies.

SYMBOLS

a	slot width, m (see fig. 13(b))
a/d	slot openness ratio
d	distance between slot center lines, m (see fig. 13(b))
H	height of test section at upstream end, m
Δh	height of step between test-section horizontal walls and model support section walls at downstream end of test section, m (see fig. 15(a))
l_1	distance from tunnel center line to wall in contraction section, m (see fig. 9(a))
l_2	distance from tunnel center line to center for corner radius in contraction section, m (see fig. 9(a))
M	Mach number
m	mass-flow rate through throat of test section, kg/sec
Δm	mass-flow rate removed from plenum, kg/sec
R	radius, m
U	mean velocity, m/sec

u root mean square of fluctuating component of velocity in streamwise direction, m/sec
 x axial or streamwise coordinate, m
 y lateral coordinate, m
 δ_f reentry flap angle measured with respect to tunnel center line, positive away from flow, deg
 θ_w test-section horizontal wall divergence angle measured with respect to tunnel center line, positive away from flow, deg

Notation:

ASME American Society of Mechanical Engineers
 DFA diffuser flow apparatus
 NTF National Transonic Facility
 TPT Langley 8-Foot Transonic Pressure Tunnel

NATIONAL TRANSONIC FACILITY

The NTF is a closed-circuit, single-return wind tunnel with a conventional fan drive capable of continuous operation. The test-section design closely resembles that of the Langley 8-Foot Transonic Pressure Tunnel, especially in the flow reentry region at the downstream end. The test section is 2.5 m square and 7.62 m long with longitudinal slots in the walls. The tunnel pressure range is from 1 to 8.85 atm (1 atm = 10.13 kPa), and the temperature range is from 78 K to 339 K. The Mach number range is from 0.1 to 1.2 with a maximum Reynolds number capability at Mach number 1.0 of 120×10^6 based on a wing chord equal to one-tenth of the test-section height (0.25 m). The drive system consists of a variable-speed fan with variable inlet guide vanes. A sketch showing the principal components of the NTF is presented in figure 1, and the NTF circuit lines are shown in figure 2.

In the cryogenic mode of operation, nitrogen is used as the test gas, with cooling accomplished by the injection of liquid nitrogen directly into the tunnel circuit. An additional mode of operation is possible at ambient temperatures using dry air or nitrogen as the test gas with cooling accomplished by a conventional chilled-water heat exchanger inside the tunnel circuit.

DIFFUSER FLOW APPARATUS

The DFA is a 0.186-scale model of the high-speed duct of the NTF. The sketch in figure 3 shows the extent of representation of the NTF by the DFA.

Essentially, the components of the NTF which were represented are a wide-angle diffuser, settling chamber, contraction section, test section, model support section, and high-speed diffuser.

There are some geometrical differences between the high-speed ducts of the NTF and the DFA. The most obvious are the inlet and exit conditions as shown in figures 3 and 4. At the upstream end, the DFA has a supply pipe, corner turn, flow conditioning chamber, and bell mouth which are not representative of the NTF. At the downstream end, there is a cylindrical section, diffuser, corner turn, and return pipe which are also not representative.

Another planned difference between the NTF and the DFA is the size of the plenum chamber surrounding the test section. A scaled model of the NTF plenum would not have been large enough to permit easy entry for access to the test section. The DFA plenum was made overscale by a factor of 1.5 on diameter to provide enough space inside it for working access to the test section.

Some other differences are less noticeable and occurred primarily because of design changes which were made to the NTF after the DFA was constructed. One such difference was a shortening of the wide-angle diffuser to about 82 percent of its original length. Another difference was a change in the corner fillets in the contraction section, from flat to circular arc. Both of these changes in the NTF design were made for structural reasons.

The number of turbulence damping screens in the NTF was increased from three to four, with a corresponding reduction in the pressure loss per screen so as to keep the overall pressure loss the same. The DFA has only three such screens.

The NTF will have a conventional chilled-water heat exchanger at the exit of the wide-angle diffuser for operation at ambient temperature. Neither the heat exchanger nor its support truss was modeled in the DFA. However, the aerodynamic effect of the heat exchanger was simulated by a combination of honeycomb and screens.

Both the contraction section and the high-speed diffuser are movable structures in the NTF to permit deployment of test-section isolation valves at the upstream and downstream ends of the plenum. The isolation valves seal the test-section plenum region to permit access to the test section without purging the entire NTF circuit. The movable structures require clearance gaps at the upstream end of the contraction section and at the downstream end of the high-speed diffuser to facilitate their movement. These gaps are not modeled in the DFA.

A schematic diagram of the DFA flow circuit is shown in figure 4. The supply pipe immediately upstream of the DFA is vented to the atmosphere to insure that the stagnation pressures in the apparatus itself will be close to atmospheric pressure. The normal stagnation temperatures vary between ambient temperature and about 310 K. The air supply is provided by two 47.2 m³/sec capacity centrifugal compressors operated in parallel. These compressors also provide plenum suction for the TPT. Drying (removal of water vapor from the air) is accomplished with the same drying circuit as is used for the TPT. This

drying circuit is powered by a 4.72 m³/sec capacity centrifugal compressor and has a 2-unit dryer. Dew point is maintained at or below 266 K. The compressor for the drying circuit is also used to provide plenum suction for the DFA when required.

In the following sections of this report, the various components of the DFA are described and compared with their counterpart in the NTF where appropriate. Experimental flow characteristics for the contraction section, the test section, and the high-speed diffuser are presented. Tunnel stations are shown in figure 5, the start of the test section being used as the reference station with the positive direction downstream.

Flow Conditioning Chamber

As may be seen in figure 4, the DFA receives its air supply from the compressors through a supply pipe which terminates in a rectangular exit that is 0.61 m wide and 2.13 m high. The flow conditioning chamber provides a relatively uniform flow to the 1.41-m-diameter circular inlet of the wide-angle diffuser. The flow conditioning treatment consists of a very wide-angle (104°), essentially two-dimensional, diffuser as shown in figure 6 with a screen and honeycomb sections installed to reduce the tendency for flow separation from the walls.

The first of three honeycombs has square cells roughly 5 cm across and 7.5 cm deep. It is formed as a cylindrical section with the upstream surface curved in a circular arc of 38-cm radius. This upstream surface has a screen placed in front of it with the screen conforming to the circular-arc curvature of the honeycomb. The screen has round wire, 0.24 mm in diameter, woven in a square mesh of about 8 wires per cm with a porosity of 0.64. This same screen material has been used throughout the DFA in either single or double layers wherever screens have been employed.

The second and third honeycombs had hexagonal cells about 1.9 cm across the flats with 0.08-mm wall thickness and 15.24-cm streamwise depth. This same honeycomb material was widely used throughout the DFA wherever honeycombs were employed. The second honeycomb was also formed in a cylindrical section with the upstream surface curved in a circular arc of about 69-cm radius. Both of the curved honeycomb surfaces had the same center of curvature which corresponded with the hypothetical apex of the straight-sided two-dimensional diffuser walls.

The downstream end of this short diffuser section had a flat third section of honeycomb. This honeycomb was backed at its downstream end with a double layer of the screen material with the orientation of the wires of the second screen rotated 45° to the wires of the first screen.

The overall streamwise length of the flow conditioning chamber is about 136 cm. In its initial configuration, as shown in figure 6(a), the chamber was rectangular, about 244 cm wide and 213 cm high at its upstream end increasing to 244 cm high at its downstream end. For increased structural integrity, the rectangular configuration was later replaced by its current configuration which

is shown in figure 6(b), a circular cylinder of nearly the same length and about 222 cm in diameter, with similar interior flow conditioning treatment.

The flow-treatment chamber is connected to the wide-angle diffuser by an axially symmetrical bell-mouth section, shown in figure 7, 0.67 m long and 1.414 m diameter at its throat. The final 15 cm of the bell mouth contains a flat honeycomb of the same material as the last two honeycombs in the flow-treatment chamber.

Wide-Angle Diffuser

The axisymmetrical wide-angle diffuser (fig. 7) immediately upstream of the settling chamber was designed in the manner described in reference 22 to have a small adverse static pressure along the walls. This small pressure gradient, with its reduced tendency for boundary-layer separation, is obtained by appropriate curvature of the walls. The centrifugal force acting on the flow as it follows the curved wall contour is balanced by the increase in pressure as the flow decelerates because of the increased area of the wide-angle diffuser. At the downstream end, the flow direction must be returned toward the axial direction. In the NTF, the turning will be accomplished by a finned-tube heat exchanger. In the DFA, the turning is accomplished by a honeycomb. The honeycomb cells are hexagonal, about 1.9 cm across flats with 0.08 mm wall thickness and 15.24 cm deep.

In addition to a downstream honeycomb or similar flow-turning device, the wide-angle diffuser also requires a downstream pressure loss in order to avoid flow separation. For the NTF, the downstream pressure loss is provided by the heat exchanger. In the DFA, this pressure loss is simulated by backing the honeycomb with two pressure loss screens. The screen wire is 0.24 mm in diameter and is woven in a square mesh of about 8 wires per cm with a resulting porosity of 0.64.

The coordinates of the wide-angle diffuser of the DFA are presented in table I. The following table shows a comparison of the geometrical characteristics of the wide-angle diffuser in the DFA and the NTF:

	DFA	NTF
Exit to inlet area ratio	2.04	2.08
Length to inlet diameter ratio	.560	.465
Exit wall angle, deg	62.8	60.6

Settling Chamber and Turbulence Damping Screens

The exit of the wide-angle diffuser is followed by a cylindrical section 2.019 m in diameter and 1.097 m long as shown in figure 7. The honeycomb with backing screens which simulate the heat exchanger are located at its upstream end. The three turbulence damping screens are spaced 11.3 cm apart, with the first screen located 45.9 cm downstream from the exit of the wide-angle diffuser. All three screens are the same, with wires 0.24 mm in diameter woven in a square mesh of about 8 wires per cm with a porosity of 0.64.

The streamline or axial component of turbulence shown in figure 8 was measured at the downstream end of the settling chamber. The measurement was made with a single sensor hot-wire probe operated in a constant temperature mode. Although the measurement was made in the settling chamber, it is plotted as a function of the Mach number in the test section. At high test-section Mach numbers, the turbulence ratio u/U is about 0.82 percent. If a turbulence reduction factor of 0.113 is assumed for the effect of the contraction (ref. 23), then the turbulence level in the test section would be predicted to be about 0.093 percent. This compares with a target level of 0.1 percent sought for the NTF (ref. 11).

Contraction Section

The DFA has an area ratio contraction of about 15 to 1. It was designed to produce uniform flow at the throat under choked conditions or, in other words, to have an essentially straight sonic line. The design area distribution for the contraction was calculated by a streamline curvature method (ref. 24) for axially symmetrical flow using the exact equations for an inviscid compressible flow.

The contraction for the DFA consists of three sections as indicated in figure 9(a) and table II. The first section is axially symmetrical with circular cross sections. The design area distribution was matched exactly in this region. The second section is a transition section where the cross-sectional shape changes from circular to square with flat corner fillets using simple geometrical fairings. Here the design area distribution is only approximately matched. The transitional cross-sections consist of quarter-round corners with flat sides. At the end of the transition section, the quarter-round corners are faired smoothly into the flat corner fillets. The third section, which is square with flat corner fillets, is continued downstream to the geometrical throat where the test section starts. The design area distribution was also matched exactly in this region.

As mentioned previously, the corner fillets in the NTF contraction are round rather than flat as in the DFA. This minor difference in fillet shape led to minor changes in the transition section, principally in the station locations for the transition section and also led to the introduction of a transition of the fillet shape from round to flat about 2.8 m upstream of the geometrical minimum in the NTF. Some of these differences may be seen by comparing the sketch of the DFA contraction (fig. 9(a)) with that of the NTF contraction (fig. 9(b)).

The Mach number distribution measured along the wall and on the center line of the DFA contraction are shown in figure 10 for a Mach number of 1.0 in the test section. Mach number distributions calculated by the stream-tube curvature method of reference 25 are shown for comparison.

Test Section and Model Support Section

The test section of the DFA, shown in the sketch of figure 11 and the photograph of figure 12, has a nominally square cross section with flat fillets at 45° angles in the corners. As noted earlier, the design of the test section closely resembles that of the TPT. Aerodynamic ventilation for the test section consists of longitudinal slots, six in the horizontal (top and bottom) walls, and two in the vertical (side) walls. The variable geometry features of the test section consist of variable wall divergence angle, variable reentry flap angle, and variable diffuser capture area.

Geometry.- The test section is 142.3 cm long. Its height and width at the upstream end are 46.38 cm. The 45° flat corner fillets are 2.83 cm high resulting in a test-section area of 2135.2 cm². The vertical walls are parallel. The horizontal walls have flexures at the upstream end permitting variable wall angles from 0.5° convergence to 1° divergence. Nominally, the horizontal wall was set at 0.38° divergence for most tests.

The plenum which surrounds the test section is 2.286 m in diameter. Compared with the NTF, the plenum of the DFA is proportionally oversized in diameter by a factor of about 1.5 and in volume by a factor of about 3.1.

Plenum suction.- As was mentioned earlier, plenum suction for the DFA is provided by using the same compressor as is used for drying the air in the circuit. The ducting for provision of plenum suction is shown in the schematic diagram of figure 4. The connection for plenum suction is at the forward end of the plenum on the left side looking upstream. The measurement of mass-flow removal is done with a calibrated ASME long-radius nozzle. A similar bell-mouth nozzle is used for mass-flow measurement when the plenum is pressurized by venting to atmospheric pressure. The inlet coordinates of the bell mouth are presented in table III.

Slots.- The planform and cross-sectional shapes of the slots, shown in figure 13, are similar on the horizontal and vertical walls, except that on the vertical walls, the slot widths are narrower in the vicinity of the reentry flaps and the beam depth behind the slotted walls is not as great as on the horizontal walls. The coordinates for the slot planform are tabulated in table IV. These shapes are provisional ones used for flow studies in the DFA and do not represent the slot shapes for the NTF.

With the exception of the downstream region where the reentry flaps are located, the maximum openness ratio of the slots on the horizontal walls is 0.1 locally. Since the physical size of the slots on the vertical walls is the same as on the horizontal walls, and since there are one-third as many slots there, the openness ratio of the vertical walls is correspondingly lower, or 0.0333 locally. If the openness of all four walls is combined (total slot

opening divided by total wall periphery) the ratio is 0.0667, excluding the contribution of the corner fillets in reducing the periphery.

Reentry flaps.- The reentry flaps (shown in fig. 14) occupy the rear 20 percent of the slot and are shaped to conform to the slot beam shape in that region. The flaps in the vertical walls (fig. 14(b)) are of constant width and are narrower than the flaps in the horizontal walls. The flap angle on the horizontal walls can be varied through a range from 4° (toward the flow) to -15° (away from the flow). Here the inward limit on flap travel is encountered when the leading edge of the flap contacts the outer edge of the slot lips. For the vertical walls, the flap-angle range is from 0° to -15° . In addition to the standard length flap, figure 14(a) also shows a long flap configuration which was used for comparison purposes in flow development and power absorption studies.

Model support section.- The model support section (figs. 11 and 15) located immediately downstream of the test section, is rectangular in cross section with corner fillets which are tapered in the streamwise direction. It is 62.18 cm long and 51.35 cm wide by 55.12 cm high at its downstream end. At its upstream end, it is 46.38 cm wide, the same width as the test section, but its height is variable. The horizontal (top and bottom) walls of the model support section are attached to flexures at their downstream end. The angle of inclination of the horizontal walls can be varied from about 0° (walls parallel to tunnel center line) to about 4.5° inward (leading edge toward flow). The difference in vertical height between the horizontal test-section walls and the horizontal model support section walls is variable from near 0 to about 3.8 cm independently on the top and bottom walls.

The hinge lines for the reentry flaps are located at the upstream end of the model support section. The hinge lines of the flaps in the horizontal walls of the test section move with the horizontal walls of the model support section. The hinge lines of the side wall flaps do not move.

The vertical walls in the model support section are contoured (table V) to relieve the blockage caused by the model support strut. The arc-sector support strut itself has a planform with a circular-arc leading edge and a swept trailing edge (fig. 15(a)), with a cross-sectional shape influenced strongly by structural requirements. The strut center body and model support sting are shown in figure 15(b). Neither the strut nor the sting in the DFA is operational hardware but both are instead dummy structural parts used to simulate the flow-field blockage and to support dummy test models for additional flow-field simulation.

Mach number distribution.- Mach number distributions measured along the center line of the DFA test section and model support section are shown in figure 16 for Mach numbers from 0.6 to 1.0 without plenum suction. For these measurements, the test-section wall divergence angle was 0.38° , the slot reentry flaps were at -2° , and the step height at the back of the test section was about 0.08 test-section half-heights.

Some effects of plenum suction on the Mach number distribution along the test-section wall are shown in figure 17 for Mach numbers of 0.8 and 1.0. The

test conditions were a wall divergence angle of 0° , a slot reentry flap angle of 0° , and gap height of about 0.08 test-section half-heights. Uniform flow was maintained to the back of the test section ($x/H = 3$) at a Mach number of 0.8 with a suction mass-flow ratio of 0.9 percent. Similar results were obtained at a Mach number of 1.0 where the optimum suction mass-flow ratio was between 2.3 and 3.3 percent. Comparable effects of plenum suction on Mach number distribution were noted in reference 26.

High-Speed Diffuser

The high-speed diffuser for the DFA, shown in figure 18, consists of two sections: a three-stage transition section and a conical section. The three stages of the transition section approximate the area distribution of a conical diffuser with a half-angle of about 2.6° which is about the same angle as the actual conical section. The transition cross-sectional shape progresses from a rectangular section with flat corner fillets to a fully round section in the three stages of nearly equal length. The flat corner fillets of the model support section are faired out within the first stage of the transition. Aside from the fillets, the shapes in the transition section consist of flat panels joined at the corners of the cross section by quarter-round conical sections. The diffuser, including the model support section, has an overall area ratio of 2.92. The high-speed diffuser is followed by a circular cylindrical duct about 1.5 m long which is used to connect the DFA to the existing return duct. (See fig. 4.)

The static-pressure recovery in the high-speed diffuser is shown in figure 19 in terms of local Mach number on the diffuser wall. In this figure, Mach number was calculated from the ratio of the local static pressure on the wall and the stagnation pressure upstream in the settling chamber. However, the local stagnation pressure of the flow in the diffuser is less than in the settling chamber because of losses between these two components and, in particular, because of rapid boundary-layer growth in the adverse pressure gradient of the diffuser. Because of this, the actual Mach number in the diffuser is not as high as is indicated in the figure, especially near the downstream end of the diffuser.

Instrumentation

The primary measurements in the DFA consisted of stagnation and static pressures and stagnation temperature. The static pressures were measured with static orifices in the walls and with a static-pressure survey tube on the tunnel center line. The stagnation pressures were measured with stagnation-pressure tubes singly or in survey rakes.

Wall static-pressure orifices in a single row have been installed in the wide-angle diffuser, settling chamber, contraction section, and high-speed diffuser. In the test section, wall static-pressure orifices were installed in both vertical walls and in the upper horizontal wall. Two of the top-wall reentry flaps and the dummy model support strut also contained orifices for the measurement of surface static pressures.

Stagnation-pressure rakes were installed in the settling chamber and at the downstream end of the high-speed diffuser. The settling-chamber rake had horizontal and vertical arms that spanned the settling chamber. Two versions of the diffuser rake were used. The first had horizontal and vertical arms that spanned the diffuser diameter. The second had an additional set of radial arms set obliquely at 45° angles to the horizontal and vertical arms and also spanned the diameter. Both diffuser rakes could be rotated about the tunnel axis to survey all parts of the diffuser exit flow.

Reference pressures for the DFA were measured in the settling chamber (stagnation pressure) and in the plenum surrounding the slotted test section (static pressure).

Chromel-alumel thermocouples for stagnation temperature measurement were located in the settling chamber, in the plenum, and at the diffuser rake station.

The pressures were measured primarily on six 48-port mechanical scanning valves with differential pressure transducers, the reference pressure corresponding either to settling chamber stagnation pressure or to plenum static pressure. A small number of individual pressure transducers were also used for special pressure measurements. The reference pressures (settling chamber stagnation pressure and plenum static pressure) were measured on automatically recording mercury manometers.

Unsteady flow measurements were made with rapid-response pressure transducers, microphones, and hot wires. Some isolated force measurements were made with strain-gage bridges.

Steady-state data were recorded on a solid-state multichannel data acquisition system. The data acquisition system was interfaced with a desk-model calculator which performed data acquisition sequencing tasks as well as providing on-line data processing capability and off-line data plotting and analysis capability through software control.

Unsteady measurements were time-averaged on root-mean-square voltmeters, or were recorded as time-history signals on oscillograph and frequency modulation tape recorders for off-line analysis.

CONCLUDING REMARKS

The diffuser flow apparatus (DFA) is essentially a wind tunnel with a 46.38-cm square test section which is operated at ambient temperature and pressure with air as the test gas. It is a 0.186-scale model of the high-speed duct of the National Transonic Facility (NTF) which is connected to an existing air supply consisting of two 47.2 m³/sec centrifugal compressors which are part of the plenum suction system for the Langley 8-Foot Transonic Pressure Tunnel. The principal NTF components which have been represented are the wide-angle diffuser, settling chamber, contraction section, test section, model support section, and high-speed diffuser.

The principal uses of the DFA have been to provide an experimental assessment of the fan pressure ratio and power requirements for the NTF and to provide verification tests for the design of the wide-angle diffuser, contraction section, and high-speed diffuser. The ability to change components of the DFA also facilitates the study of test section slot shaping requirements and flow generation characteristics.

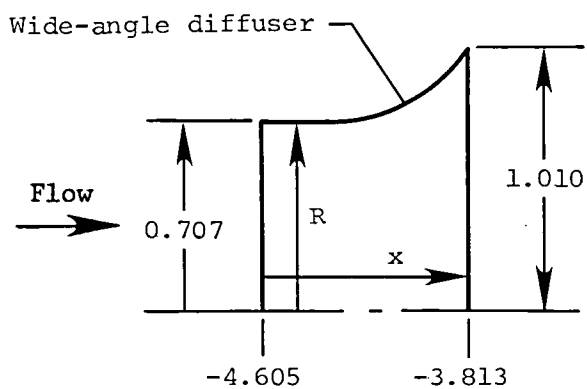
Langley Research Center
National Aeronautics and Space Administration
Hampton, VA 23665
March 19, 1981

REFERENCES

1. Heppe, Richard R.; O'Laughlin, B. D.; and Celniker, Leo: New Aeronautical Facilities - We Need Them Now. *Astronaut. & Aeronaut.*, vol. 6, no. 3, Mar. 1968, pp. 42-54.
2. Howe, John T., ed.: Some Fluid Mechanical Problems Related to Subsonic and Supersonic Aircraft. NASA SP-183, 1968.
3. Lukasiwicz, Julius: The Need for Developing a High Reynolds Number Transonic Wind Tunnel in the U.S. *Astronaut. & Aeronaut.*, vol. 9, no. 4, Apr. 1971, pp. 64-70.
4. Transonic Aerodynamics. AGARD CP No. 35, Sept. 1968.
5. Facilities and Techniques for Aerodynamic Testing at Transonic Speeds and High Reynolds Number. AGARD Conf. Pre-Print No. 83, Aug. 1971.
6. The Need for Large Wind Tunnels in Europe. AGARD-AR-60, Dec. 1972.
7. Goodyer, Michael J.; and Kilgore, Robert A.: High-Reynolds-Number Cryogenic Wind Tunnel. *AIAA J.*, vol. 11, no. 5, May 1973, pp. 613-619.
8. Margoulis, W.: A New Method of Testing Models in Wind Tunnels. NACA TN 52, 1921.
9. Smelt, R.: Power Economy in High-Speed Wind Tunnels by Choice of Working Fluid and Temperature. Rep. No. Aero. 2081, British R.A.E., Aug. 1945.
10. McKinney, Linwood W.; and Howell, Robert R.: The Characteristics of the Planned National Transonic Facility. Proceedings - AIAA. The Aerodynamic Testing Conference, June 1976, pp. 176-184.
11. Howell, Robert R.; and McKinney, Linwood W.: The U.S. 2.5-Meter Cryogenic High Reynolds Number Tunnel. High Reynolds Number Research, Donald D. Baals, ed., NASA CP-2009, 1977, pp. 27-51. (Also available as ICAS Paper No. 76-04.)
12. Baals, Donald D.: Design Considerations of the National Transonic Facility. *Advances in Engineering Science - Volume 4*, NASA CP-2001, [1976], pp. 1583-1602.
13. Nicks, Oran W.; and McKinney, Linwood W.: Status and Operational Characteristics of the National Transonic Facility. AIAA Paper 78-770, Apr. 1978.
14. Kilgore, R. A.; Igoe, W. B.; Adcock, J. B.; Hall, R. M.; and Johnson, C. B.: Full Scale Aircraft Simulation With Cryogenic Tunnels and Status of the National Transonic Facility. First International Symposium on Cryogenic Wind Tunnels, Dep. Aeronaut. & Astronaut., Univ. Southampton, Apr. 1979, pp. 11.1 - 11.19. (Also available as NASA TM-80085.)

15. Kilgore, Robert A.: Development of the Cryogenic Tunnel Concept and Application to the U.S. National Transonic Facility. Towards New Transonic Windtunnels, AGARD-AG-240, Nov. 1979, pp. 2-1 - 2-27.
16. Howell, Robert R.: Overview of Engineering Design and Operating Capabilities of the National Transonic Facility. Cryogenic Technology. NASA CP-2122, Pt. I, 1980, pp. 49-75.
17. Howell, Robert R.: The National Transonic Facility: Status and Operational Planning. A Collection of Technical Papers - AIAA 11th Aerodynamic Testing Conference, Mar. 1980, pp. 1-9. (Available as AIAA-80-0415.)
18. Igoe, William B.: Characteristics and Status of the U.S. National Transonic Facility. Cryogenic Wind Tunnels, AGARD-LS-111, July 1980, pp. 17-1 - 17-11.
19. Hartzuiker, J. P.; and North, R. J.: The European Transonic Windtunnel ETW. Cryogenic Wind Tunnels, AGARD-LS-111, July 1980, pp. 16-1 - 16-17.
20. Stokes, George M.: Description of a 2-Foot Hypersonic Facility at the Langley Research Center. NASA TN D-939, 1961.
21. Gloss, Blair B.: Plenum Response to Simulated Disturbances of the Model and Fan Inlet Guide Vanes in a Transonic Tunnel. NASA TM-81869, 1980.
22. Küchemann, Dietrich; and Weber, Johanna: Aerodynamics of Propulsion. First ed. McGraw-Hill Book Co., Inc., 1953, pp. 247-278.
- X 23. Beckwith, I. E.; and Rotta, J. C.: Appendix 7 - Effects of Contractions on Turbulence in the Working Section. A Further Review of Current Research Aimed at the Design and Operation of Large Wind Tunnels, AGARD-AR-83, Sept. 1975, pp. 113-117.
- X 24. Barger, Raymond L.: Streamline Curvature Design Procedure for Subsonic and Transonic Ducts. NASA TN D-7368, 1973. *Vol. 1192C 864-2318 2a 113*
- X 25. Ferguson, D. R.; and Keith, J. S.: Modifications to the Streamtube Curvature Program. Volume I - Program Modifications and User's Manual. NASA CR-132705, 1975.
26. Goethert, Bernhard H.: Transonic Wind Tunnel Testing. AGARDograph No. 49, Pergamon Press, 1961.

TABLE I.- WIDE-ANGLE DIFFUSER COORDINATES



x, m	R, m
-4.605	0.707
-4.548	.708
-4.492	.711
-4.435	.715
-4.438	.720
-4.322	.726
-4.280	.733
-4.237	.741
-4.195	.750
-4.153	.761
-4.124	.769
-4.096	.779
-4.068	.789
-4.040	.802
-4.011	.815
-3.983	.813
-3.962	.843
-3.941	.858
-3.919	.889
-3.898	.892
-3.884	.905
-3.870	.920
-3.856	.936
-3.842	.955
-3.835	.965
-3.827	.978
-3.823	.986
-3.818	.995
-3.813	1.010

TABLE II.- COORDINATE PARAMETERS FOR CONTRACTION SECTION

[l_1 , l_2 , and R are defined in figure 9(a)]

Full radius from station -2.716 to -2.207

Station, m	l_1 , m
-2.716	1.008
-2.662	1.007
-2.609	1.004
-2.557	1.001
-2.506	.996
-2.455	.989
-2.404	.980
-2.355	.967
-2.306	.952
-2.261	.936
-2.216	.917
-2.207	.914

Transition from full radius to square section

from station -2.207 to -1.744

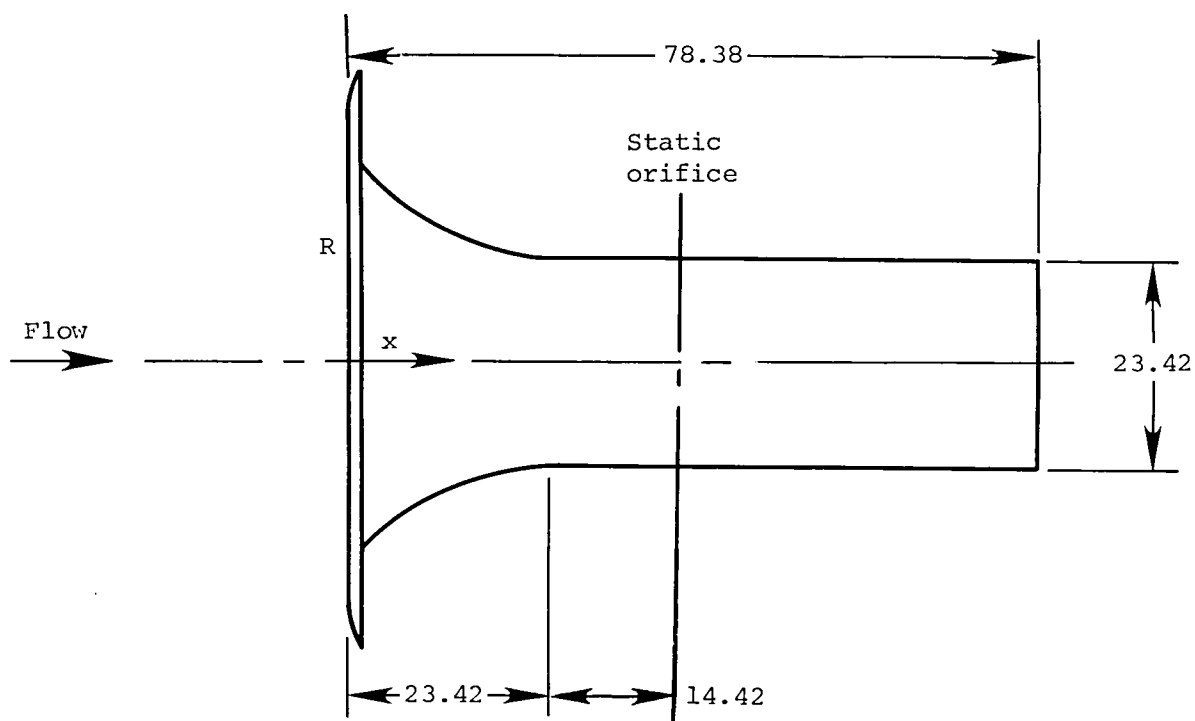
Station, m	l_1 , m	l_2 , m	R, m
-2.207	0.914	0	0.914
-2.157	.871	.052	.819
-2.106	.828	.103	.725
-2.056	.785	.155	.631
-2.006	.743	.206	.536
-1.955	.700	.258	.442
-1.905	.657	.310	.348
-1.855	.614	.361	.253
-1.805	.572	.413	.159
-1.754	.529	.464	.064
-1.744	.525	.461	0

TABLE II.- Concluded

Flat corner fillets begin at station -1.754 and end at station 0

Station, m	l_1 , m	l_2 , m	Station, m	l_1 , m	l_2 , m
-1.744	0.525	0.461	-0.931	0.290	0.255
-1.727	.515	.453	-.906	.287	.249
-1.709	.506	.444	-.881	.283	.249
-1.691	.497	.436	-.856	.280	.246
-1.673	.488	.428	-.847	.278	.244
-1.654	.479	.420	-.831	.277	.243
-1.635	.470	.413	-.806	.274	.240
-1.614	.462	.406	-.780	.271	.238
-1.596	.454	.399	-.755	.268	.235
-1.576	.446	.392	-.729	.266	.233
-1.556	.438	.385	-.704	.263	.231
-1.535	.431	.378	-.678	.260	.229
-1.515	.423	.372	-.652	.258	.227
-1.493	.416	.365	-.627	.256	.225
-1.472	.409	.359	-.601	.254	.223
-1.451	.402	.353	-.575	.252	.221
-1.429	.395	.347	-.549	.250	.219
-1.407	.389	.341	-.523	.248	.218
-1.385	.382	.336	-.498	.247	.216
-1.362	.376	.330	-.472	.245	.215
-1.340	.370	.325	-.446	.243	.214
-1.317	.364	.320	-.420	.242	.213
-1.293	.359	.315	-.394	.241	.211
-1.270	.353	.310	-.368	.240	.210
-1.247	.348	.305	-.342	.238	.209
-1.224	.342	.301	-.315	.237	.209
-1.200	.337	.296	-.289	.237	.208
-1.176	.332	.292	-.263	.236	.207
-1.152	.327	.287	-.237	.235	.206
-1.128	.323	.283	-.211	.234	.206
-1.104	.318	.279	-.185	.234	.205
-1.080	.314	.275	-.158	.233	.205
-1.055	.309	.272	-.132	.233	.204
-1.031	.305	.268	-.106	.232	.204
-1.006	.301	.265	-.080	.232	.204
-.981	.297	.261	-.053	.232	.204
-.956	.294	.258	-.027	.232	.204

TABLE III.- BELL-MOUTH INLET COORDINATES



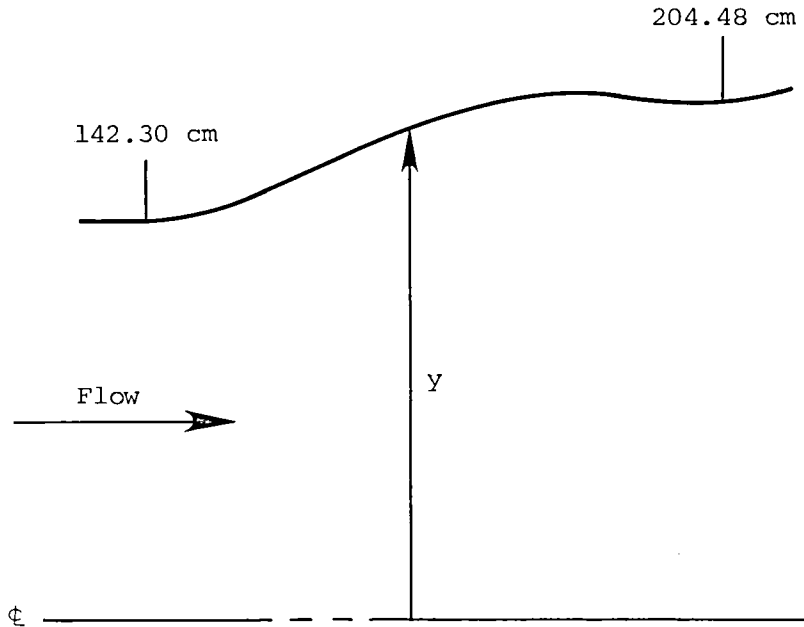
$x, \text{ cm}$	$R, \text{ cm}$
0	27.33
.13	25.73
.51	24.10
1.12	22.50
2.06	20.93
3.30	19.30
4.95	17.70
7.11	16.13
9.02	15.01
11.41	13.97
13.82	13.00
16.23	12.47
18.62	12.04
21.03	11.79
23.42	11.71

TABLE IV.- SLOT COORDINATES

[a is slot width; d is distance between slots
 (7.73 cm for horizontal walls, 23.19 cm for
 vertical walls)]

Station x, m	Horizontal wall a/d	Vertical wall a/d
0	0	0
.0095	0	0
.0464	.0145	.0048
.0927	.0276	.0092
.1391	.0401	.0134
.1855	.0519	.0173
.2319	.0624	.0208
.2782	.0722	.0241
.3246	.0802	.0267
.3710	.0874	.0291
.4173	.0933	.0311
.4637	.0979	.0326
.5101	.1000	.0333
1.0948	.1000	.0333

TABLE V.- MODEL SUPPORT SECTION VERTICAL WALL COORDINATES



x, cm	y, cm	x, cm	y, cm
142.30	23.19	165.25	25.00
142.86	23.20	166.33	25.11
143.54	23.21	167.68	25.24
144.05	23.22	168.82	25.35
144.73	23.24	169.55	25.40
145.97	23.30	171.93	25.51
147.33	23.38	173.91	25.54
148.69	23.49	175.38	25.55
150.27	23.64	177.58	25.56
151.74	23.78	179.90	25.57
152.76	23.89	182.10	25.57
154.17	24.02	184.42	25.58
155.41	24.14	186.69	25.59
157.28	24.30	188.89	25.60
158.58	24.40	191.55	25.61
159.77	24.49	193.13	25.61
160.62	24.55	196.07	25.62
161.29	24.61	199.01	25.64
162.09	24.67	201.39	25.65
162.59	24.72	203.65	25.65
163.50	24.81	204.48	25.68
164.29	24.09		

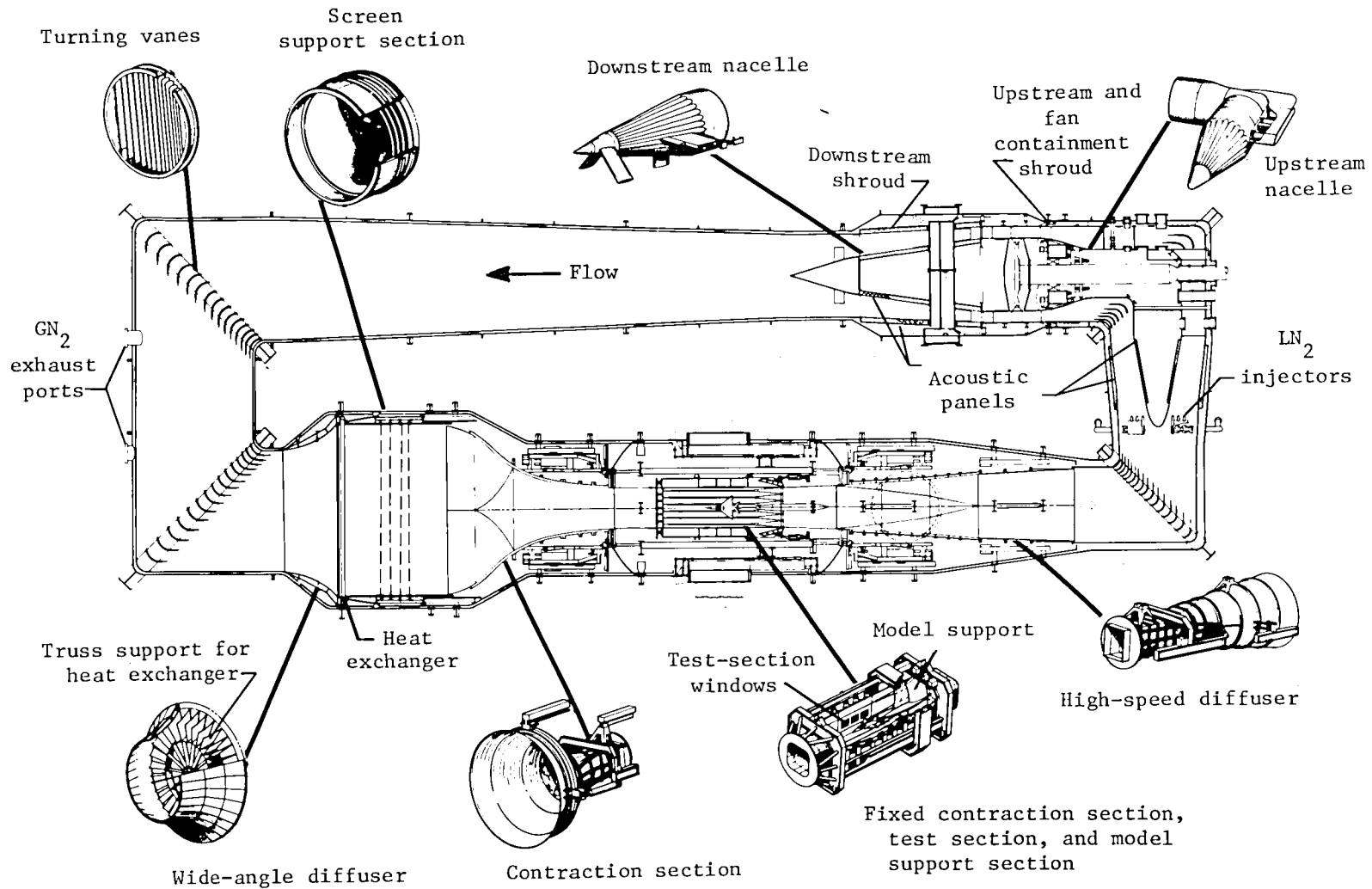


Figure 1.- Plan view of NTF circuit showing various components.

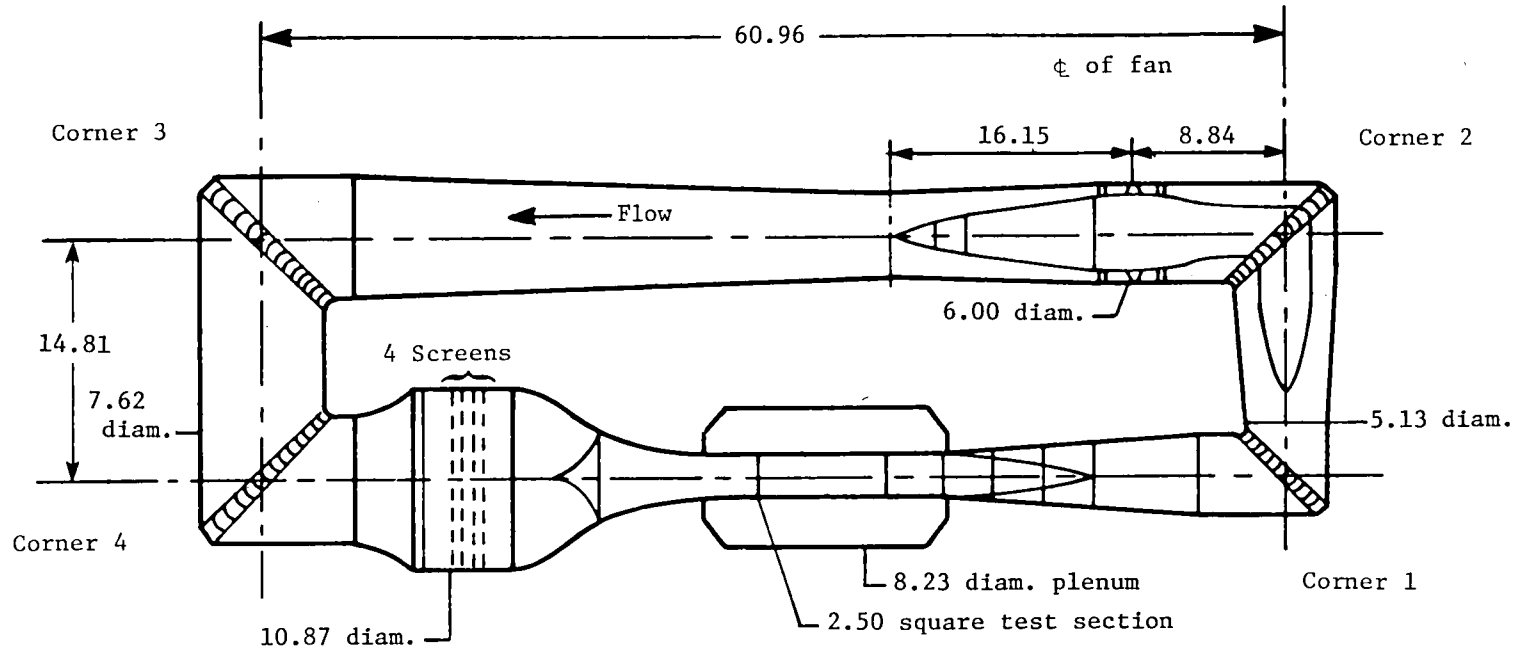


Figure 2.- NTF circuit lines. Dimensions are in meters.

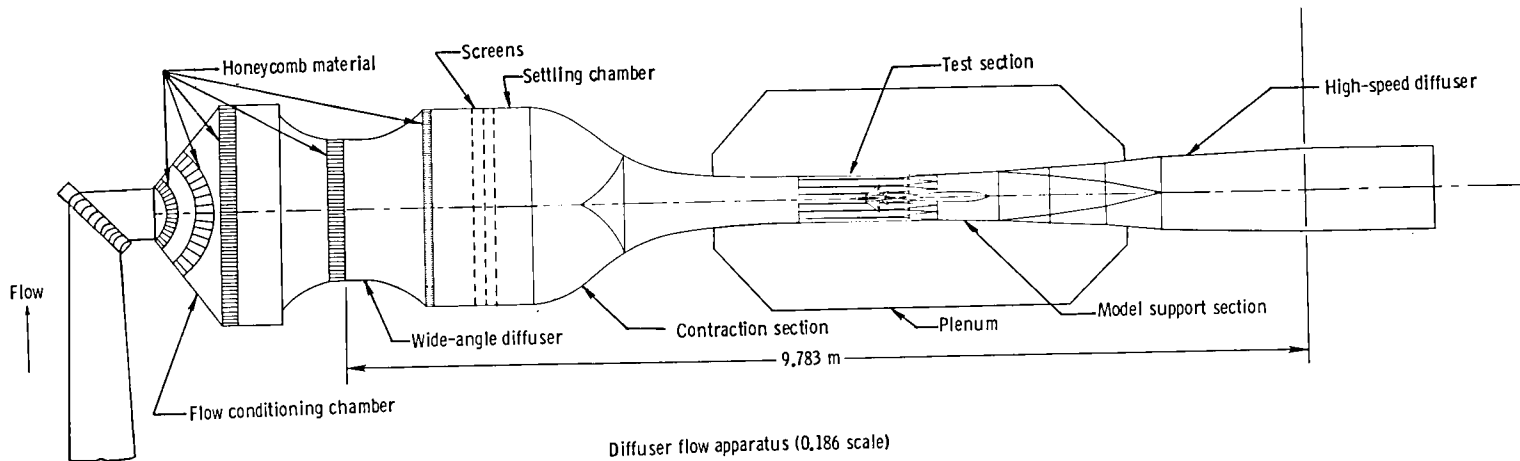
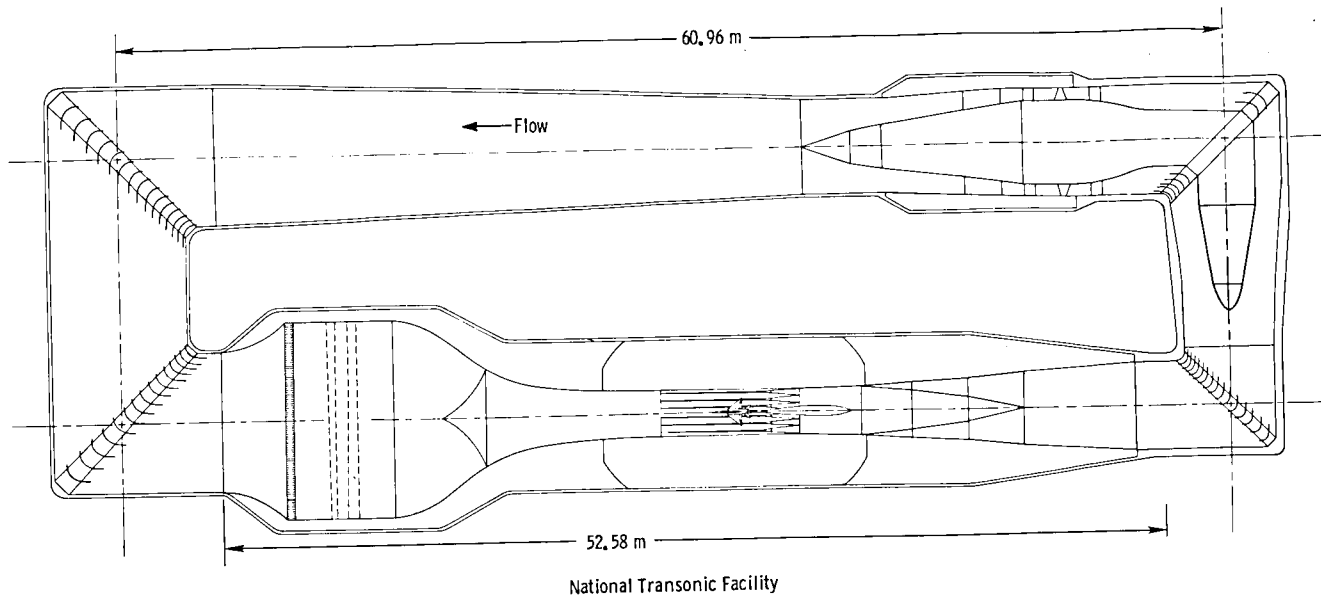


Figure 3.- Comparison showing extent of representation of NTF by DFA.

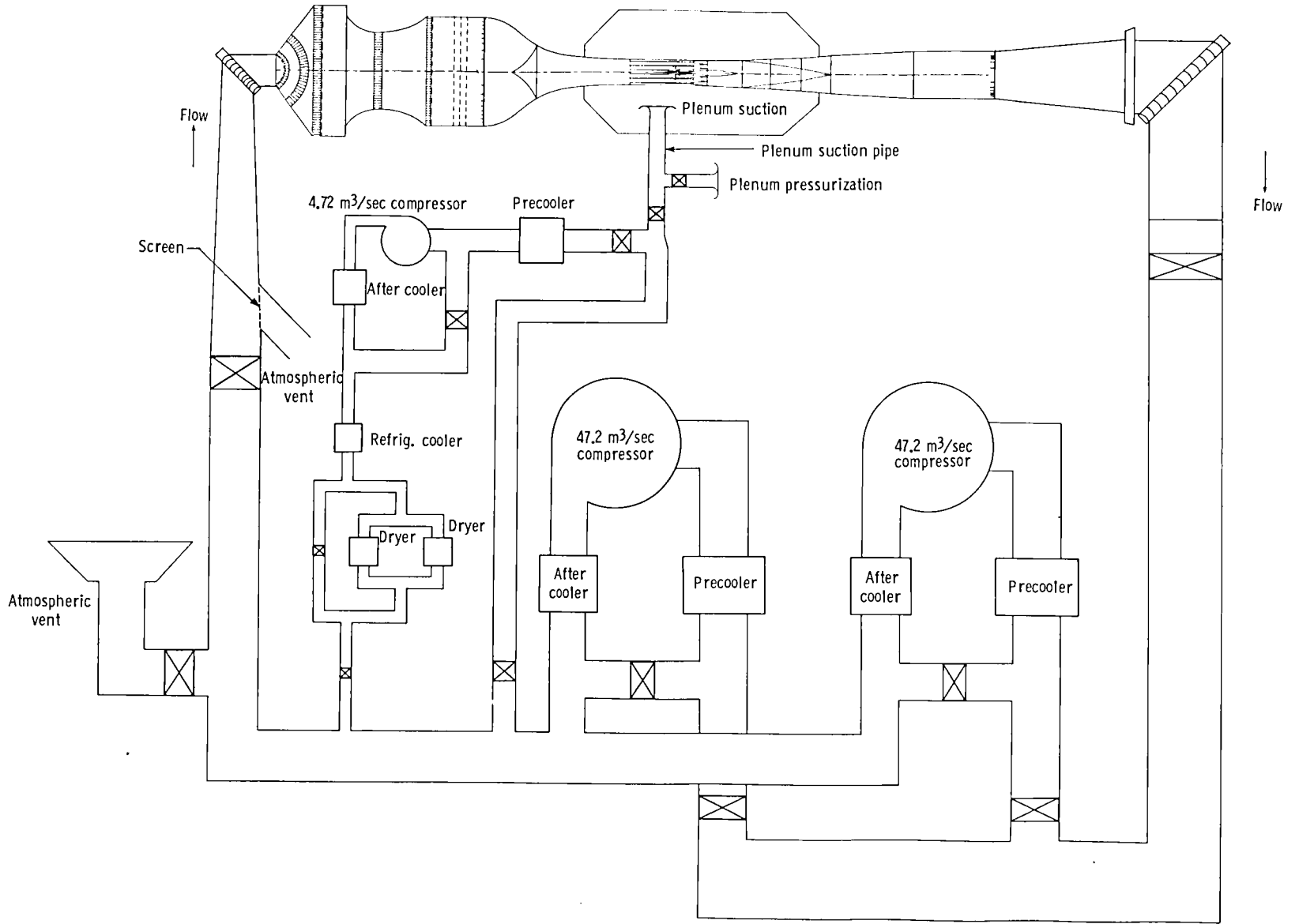


Figure 4.- Schematic diagram of DFA flow circuit.

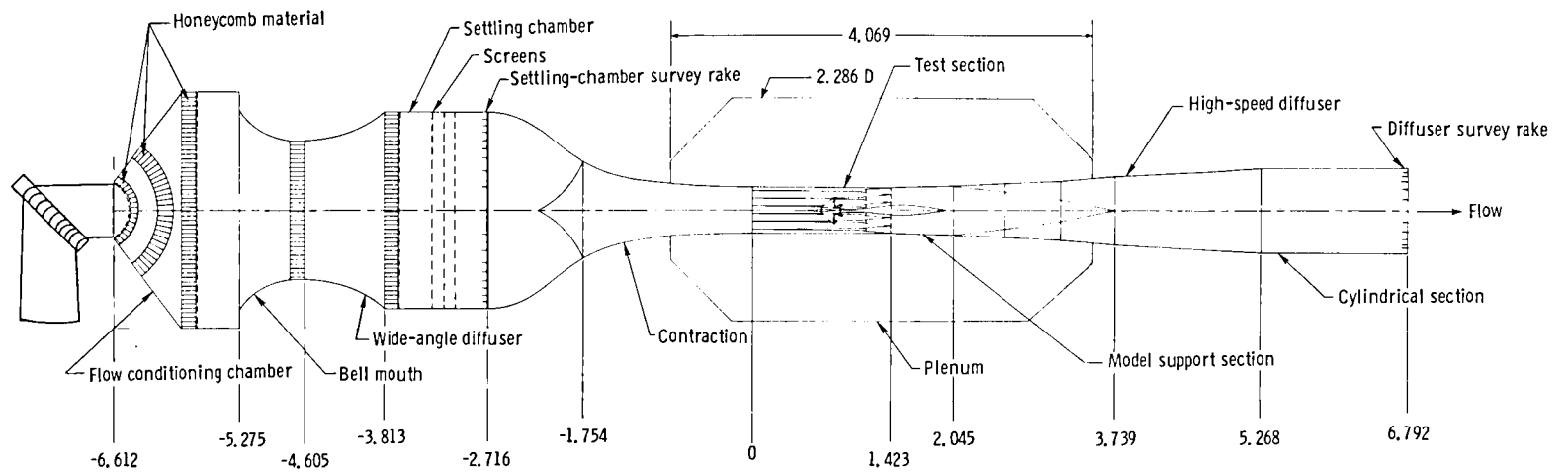
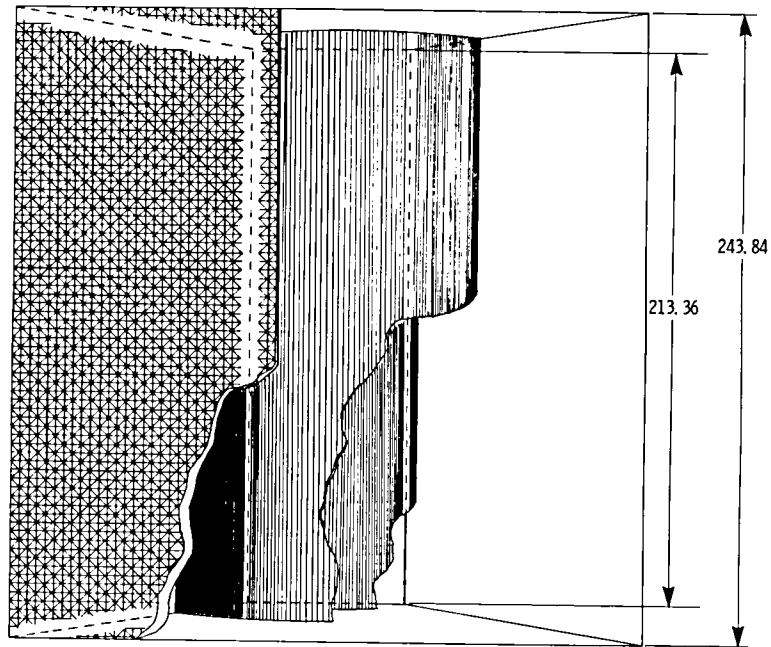
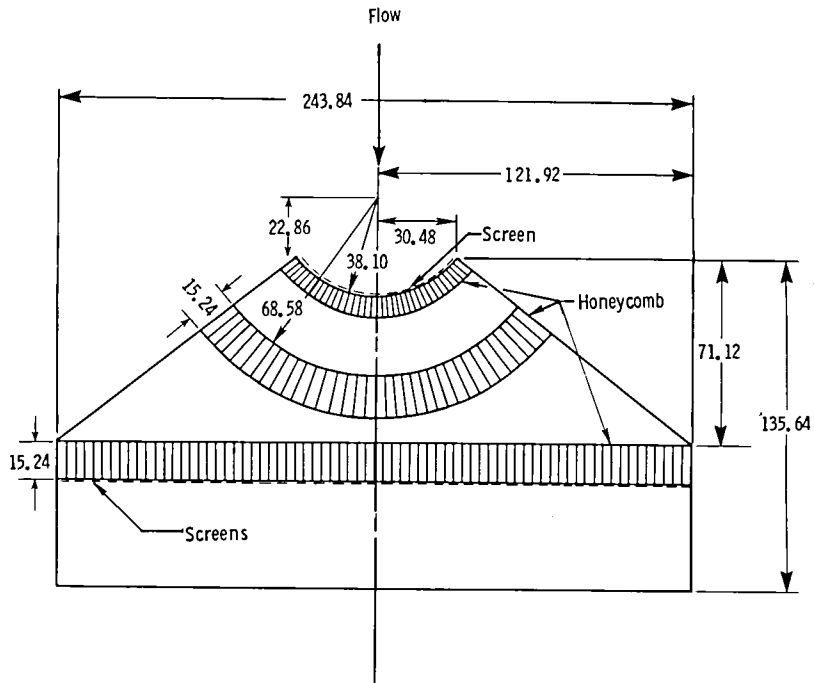
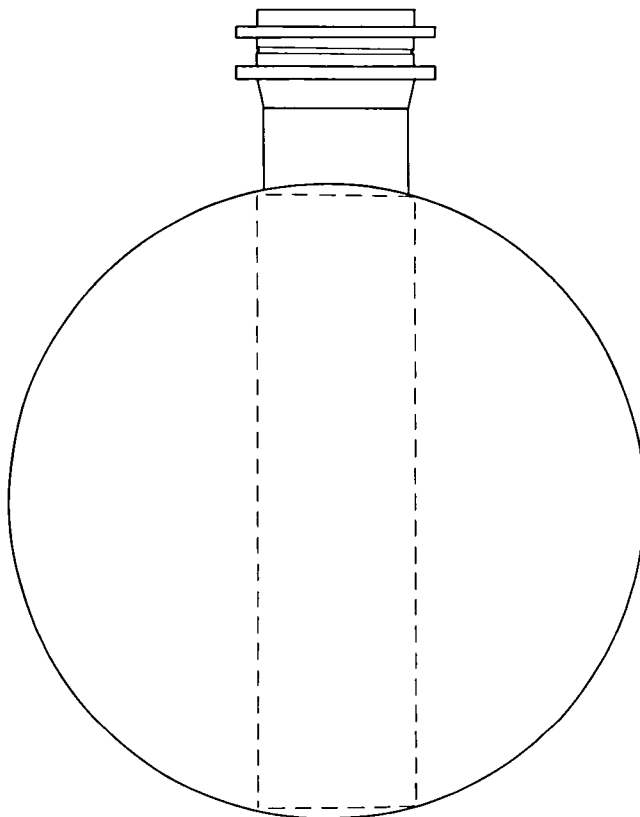
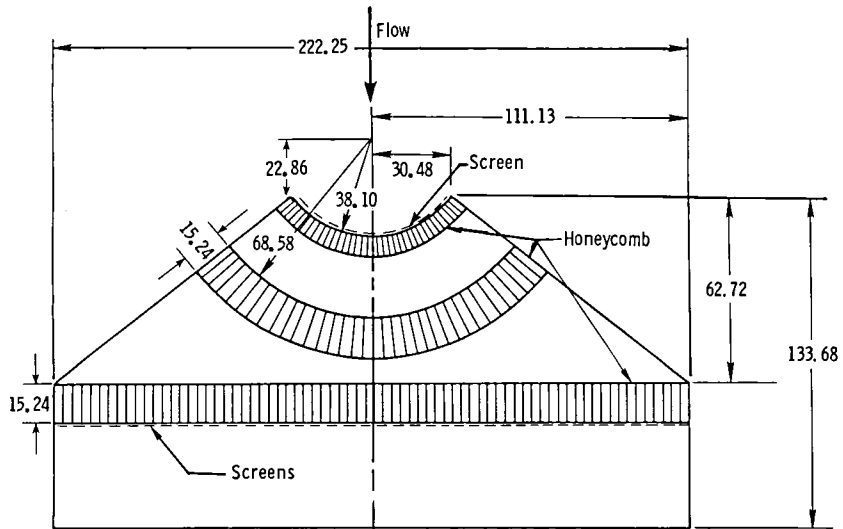


Figure 5.- Section designation and tunnel stations for DFA. All dimensions are in meters.



(a) Rectangular configuration.

Figure 6.- Flow conditioning chamber for DFA. All dimensions are in centimeters.



(b) Cylindrical configuration.

Figure 6.- Concluded.

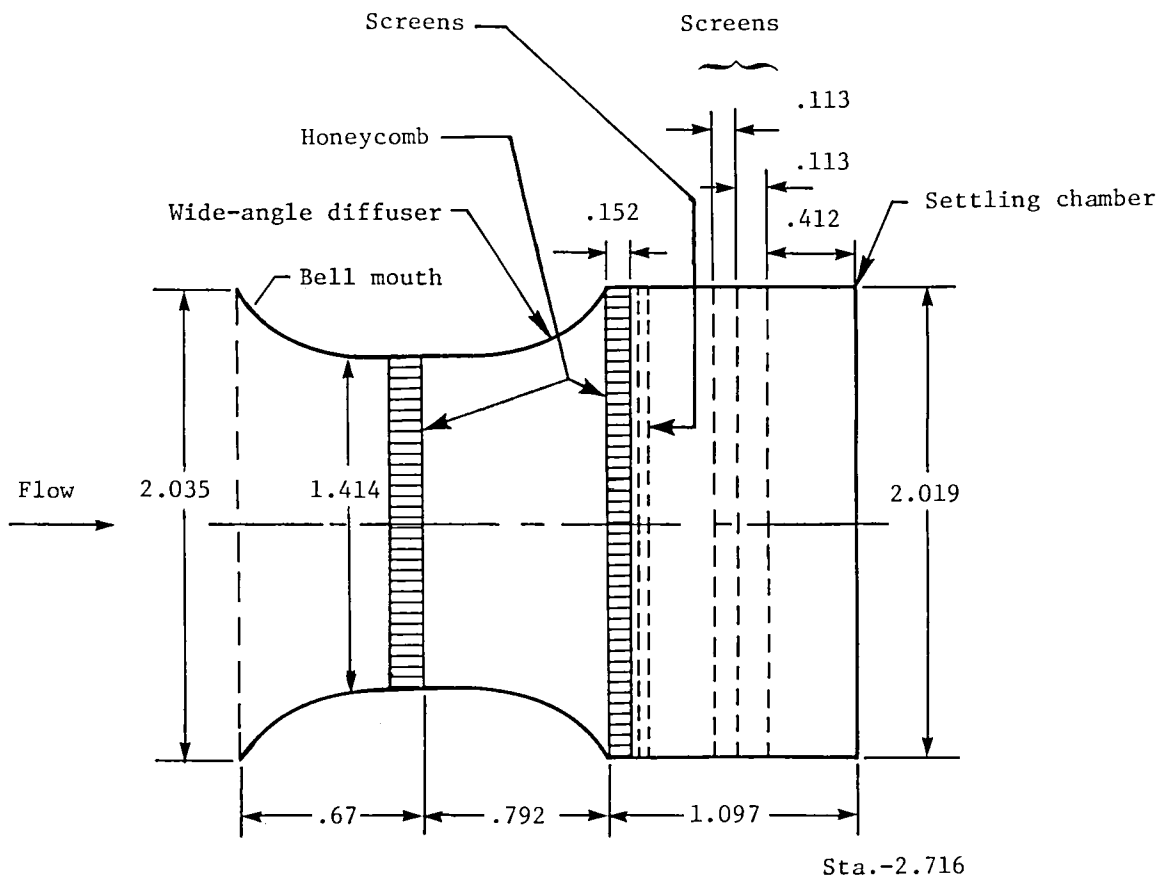


Figure 7.- Sketch of bell mouth, wide-angle diffuser, and settling chamber of DFA. All dimensions are in meters.

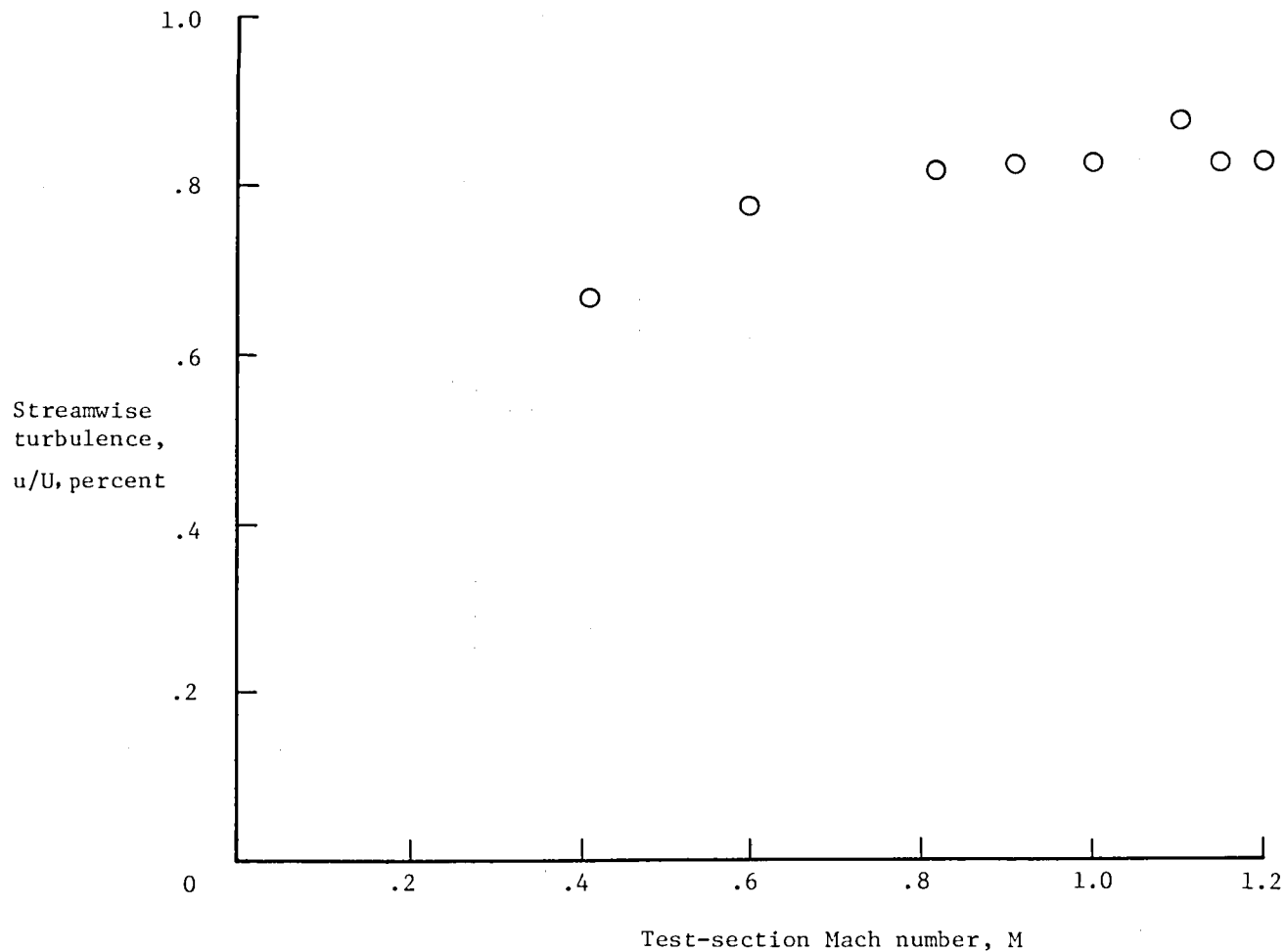
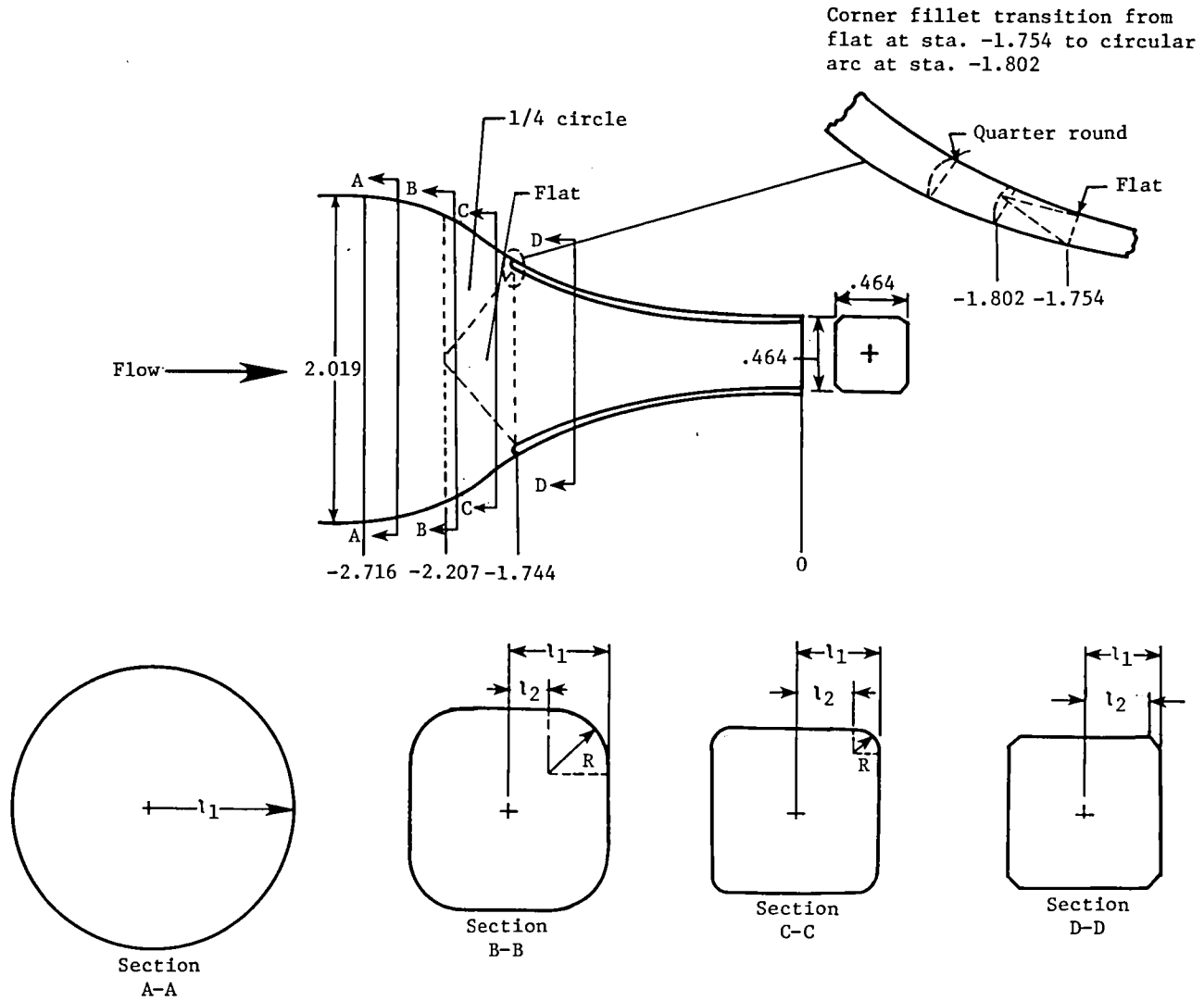
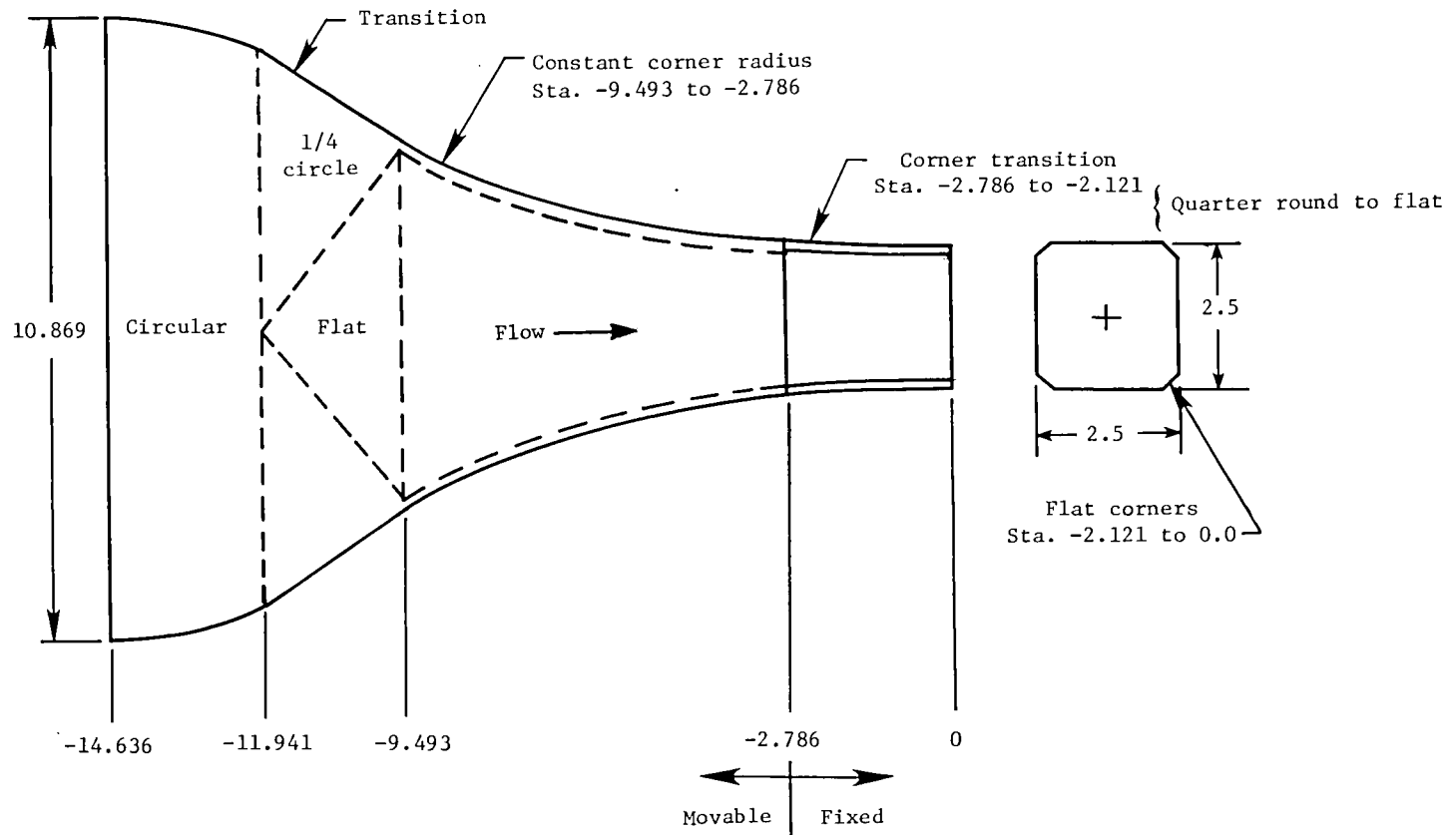


Figure 8.- Streamwise component of turbulence measured in settling chamber.



(a) Contraction section of DFA.

Figure 9.- Contraction sections of DFA and NTF. All dimensions are in meters.



(b) Design shape for contraction section of NTF.

Figure 9.- Concluded.

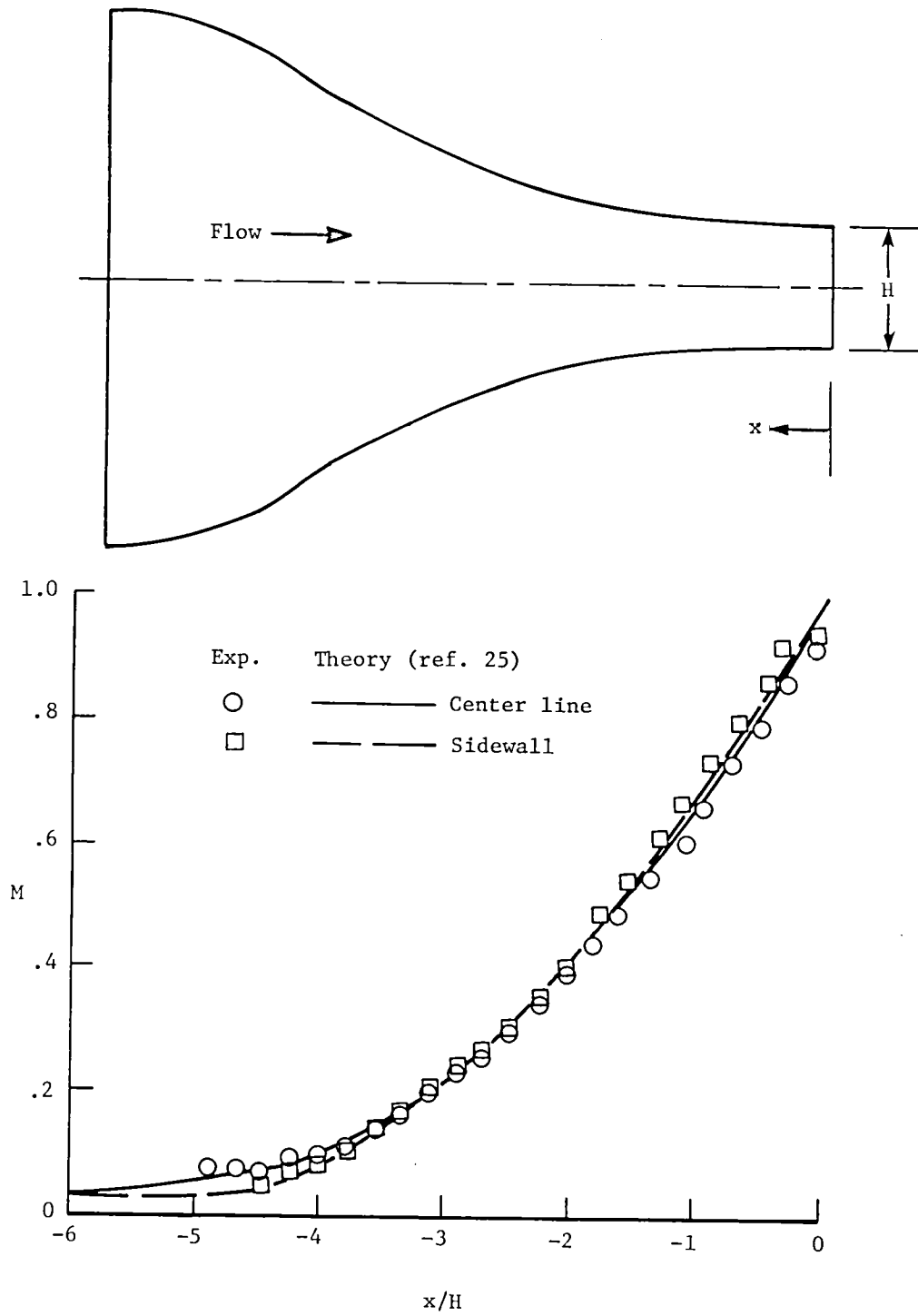


Figure 10.- Mach number distribution along wall and center line of DFA contraction section for a test-section Mach number of 1.0.

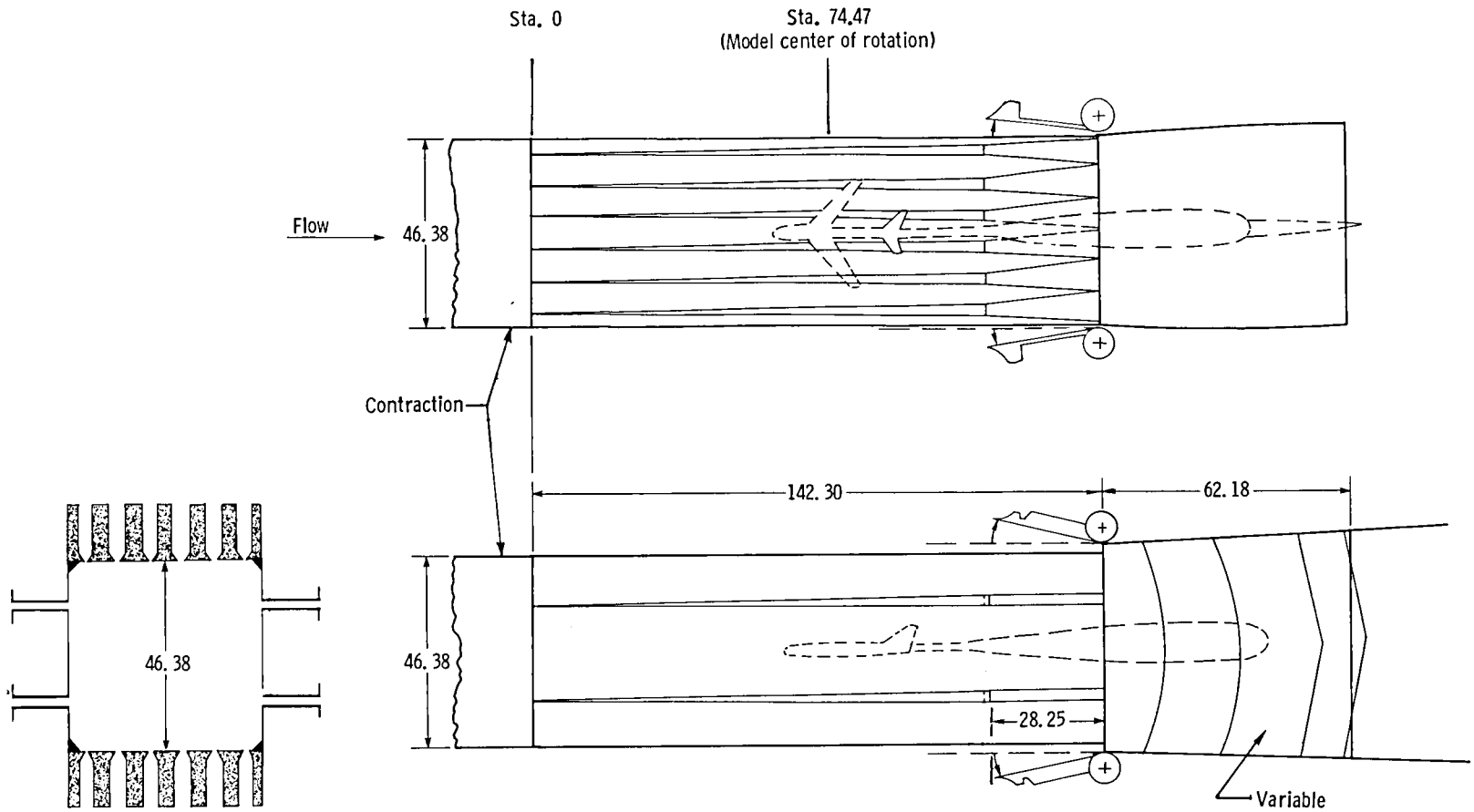
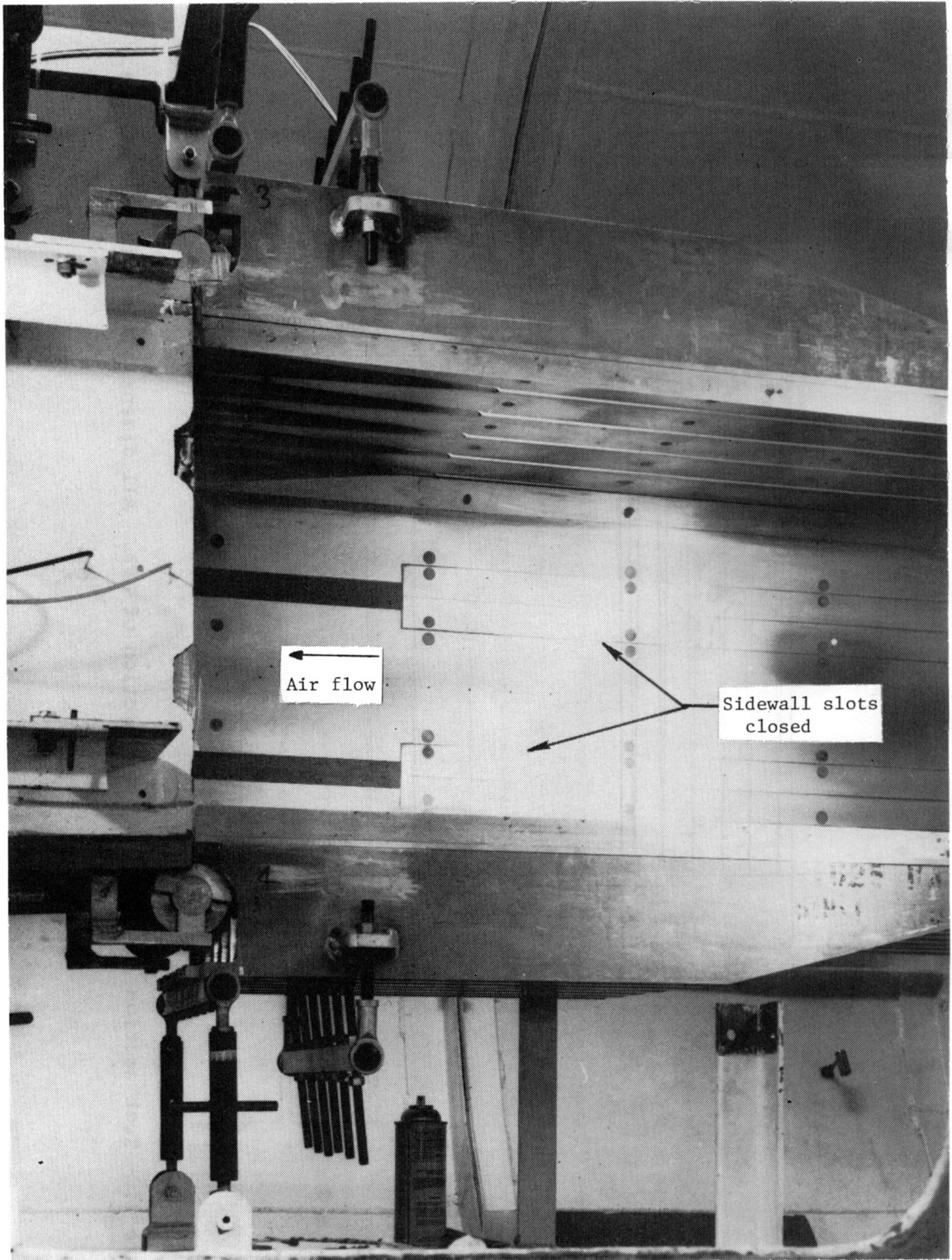
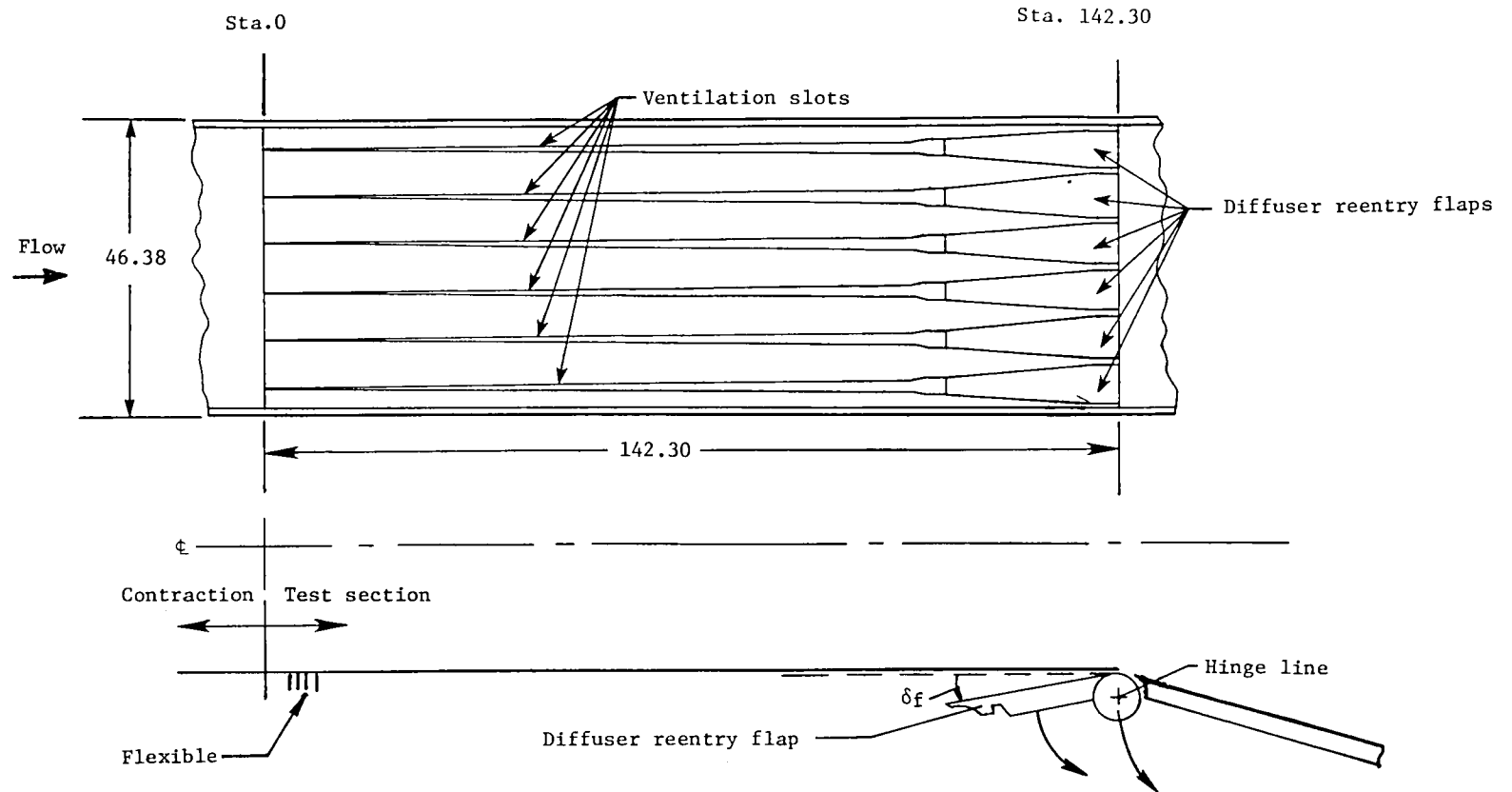


Figure 11.- Test section and model support section of DFA. All dimensions are in centimeters.



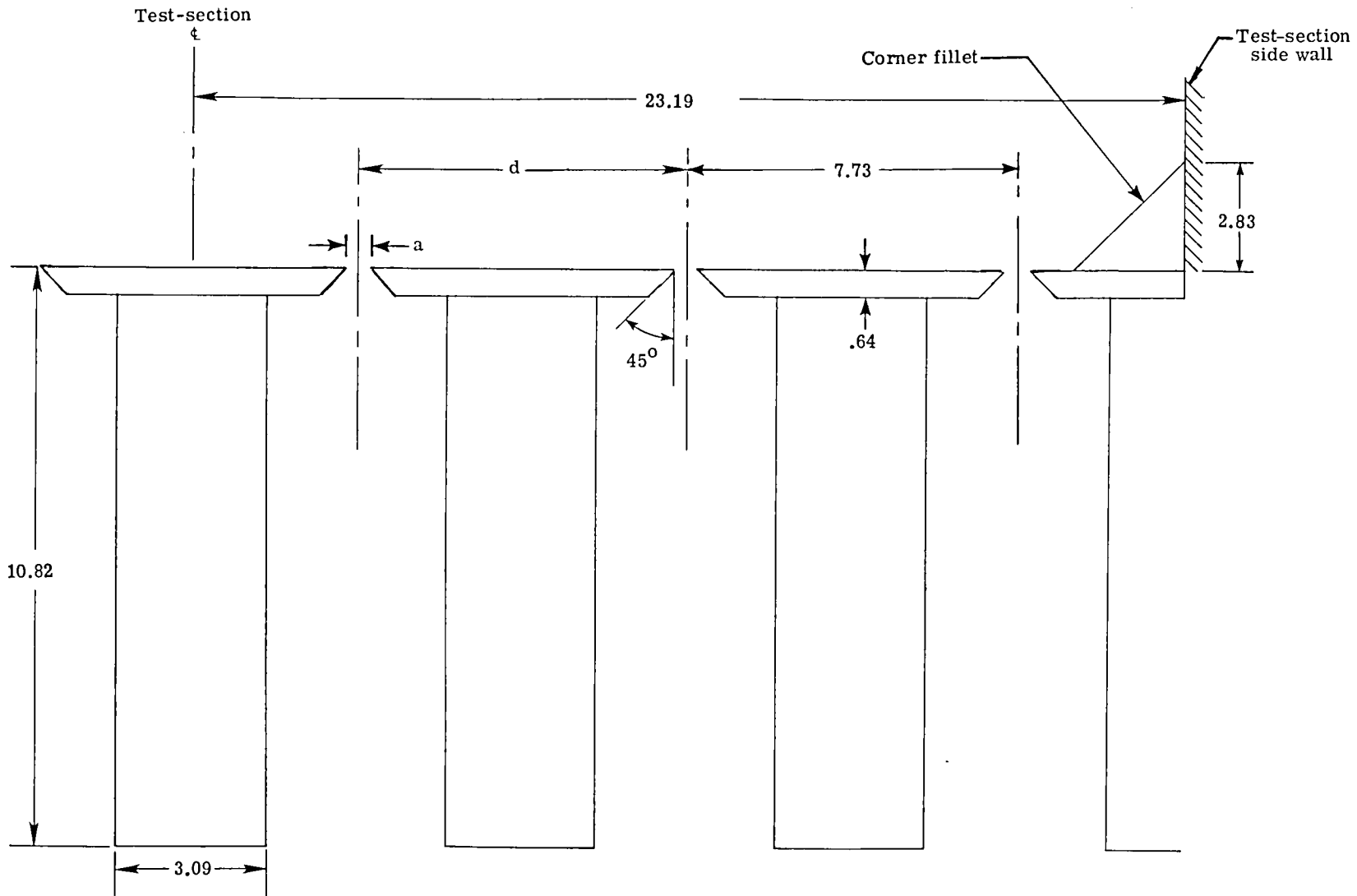
L-75-6707.1

Figure 12.- DFA test section installed in plenum (sidewall slots closed).

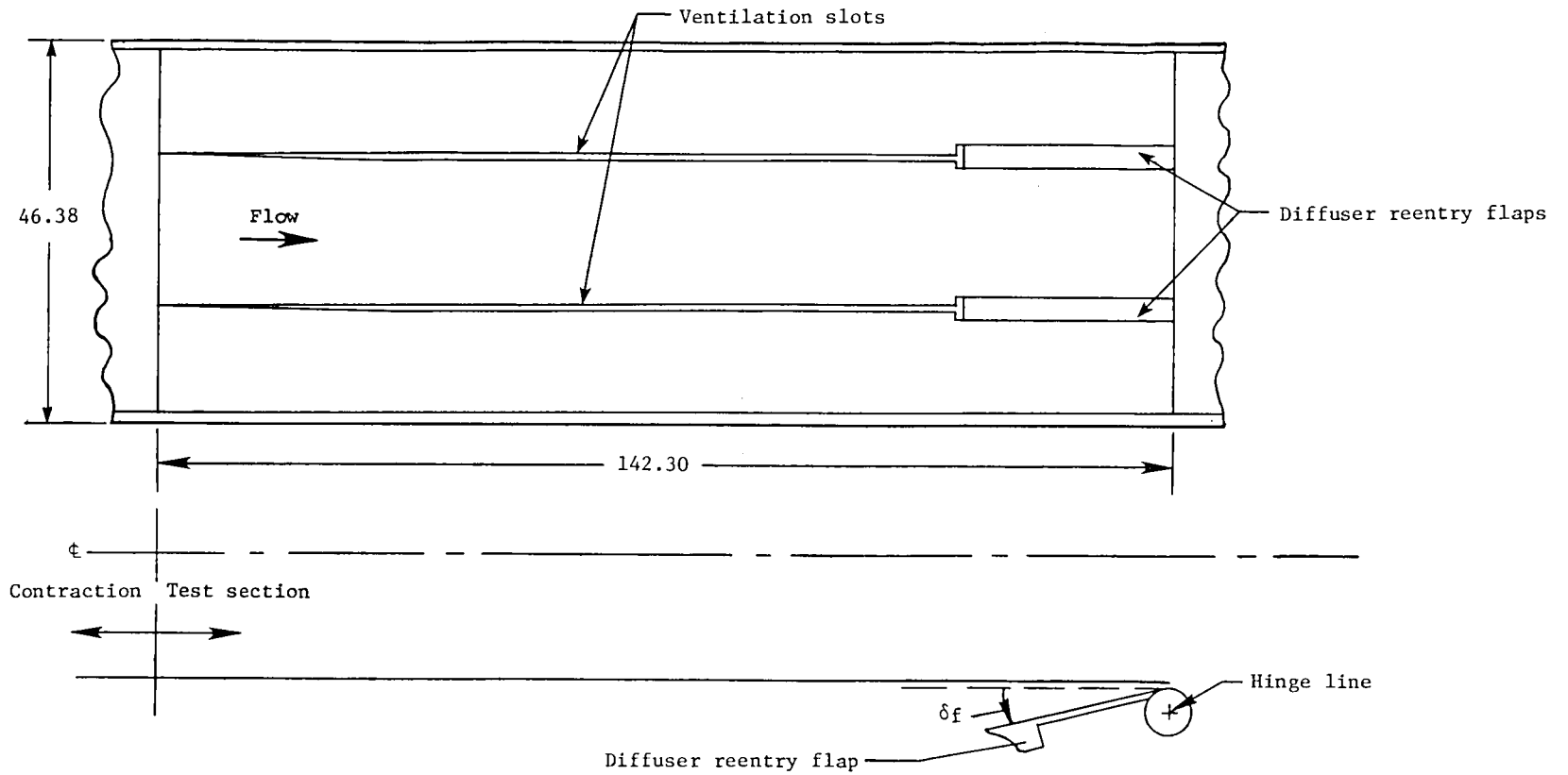


(a) Slot planform shape on horizontal walls.

Figure 13.- Planform and cross-sectional shapes of test section slots of DFA.
All dimensions are in centimeters.

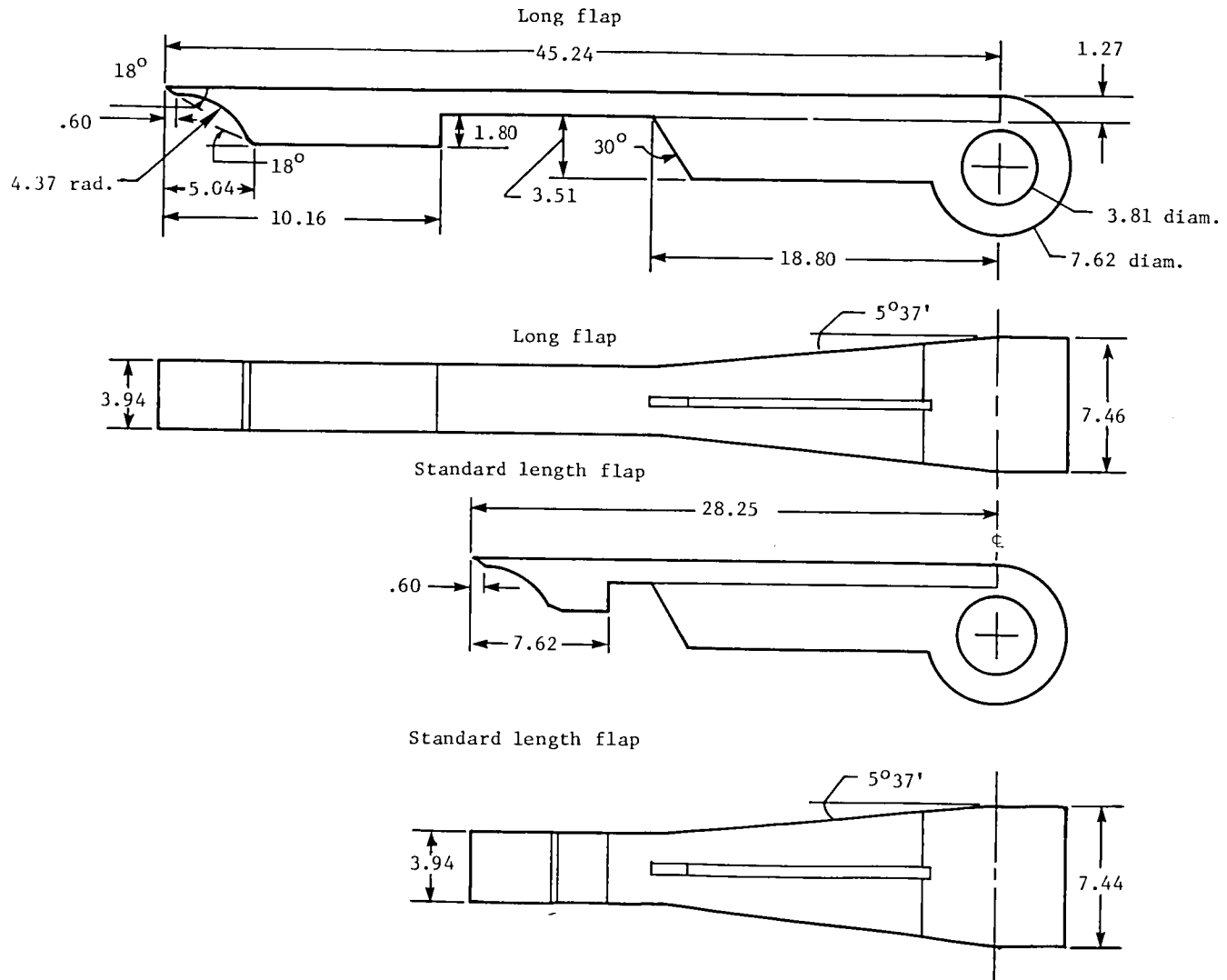


(b) Slot cross-sectional shape on horizontal walls.



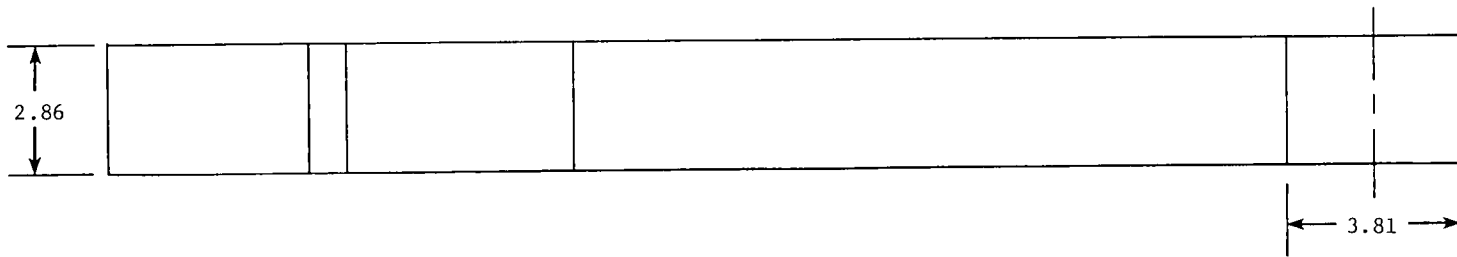
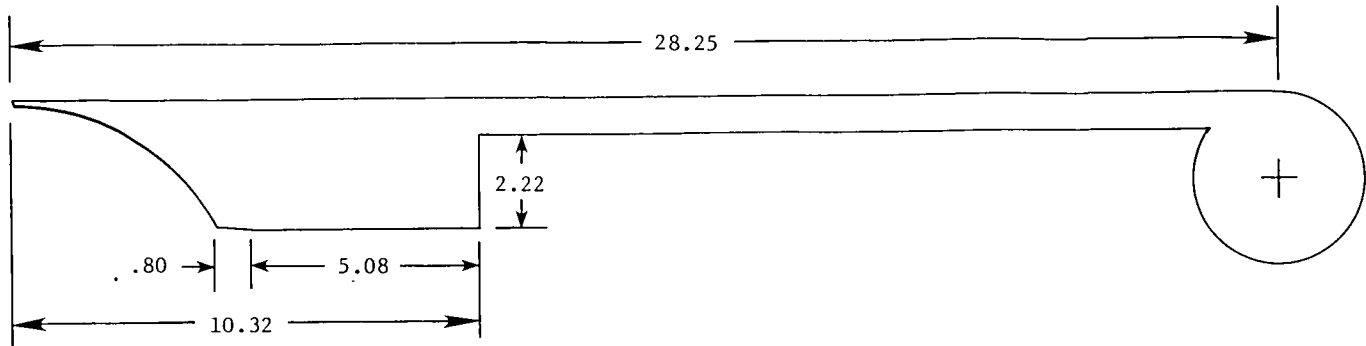
(c) Slot planform shape on vertical walls.

Figure 13.- Concluded.



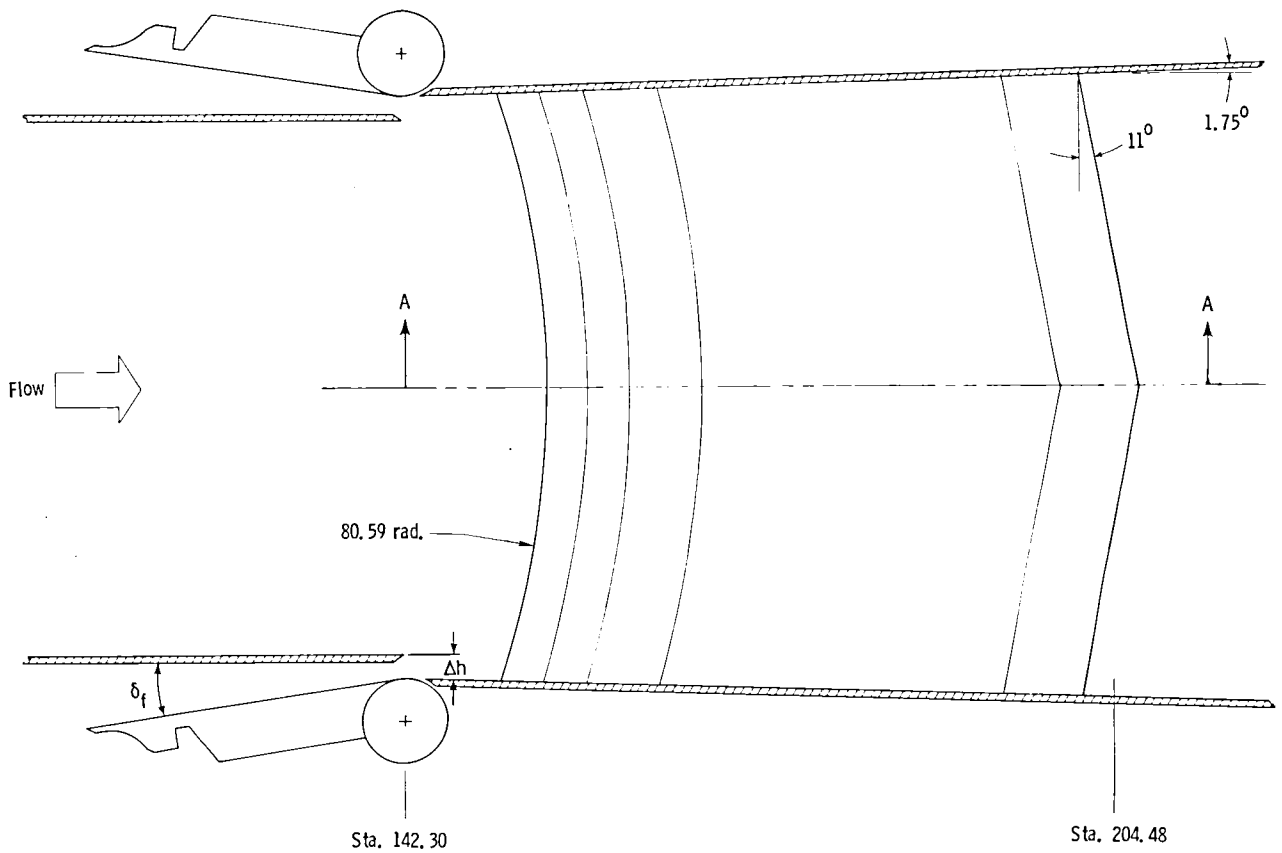
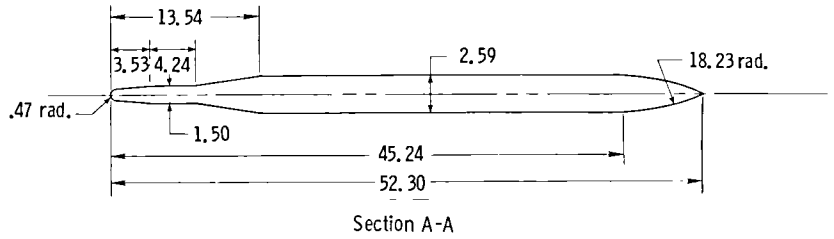
(a) Standard length and long flaps for horizontal-wall slots.

Figure 14.- Details of diffuser reentry flaps of DFA. All dimensions are in centimeters.



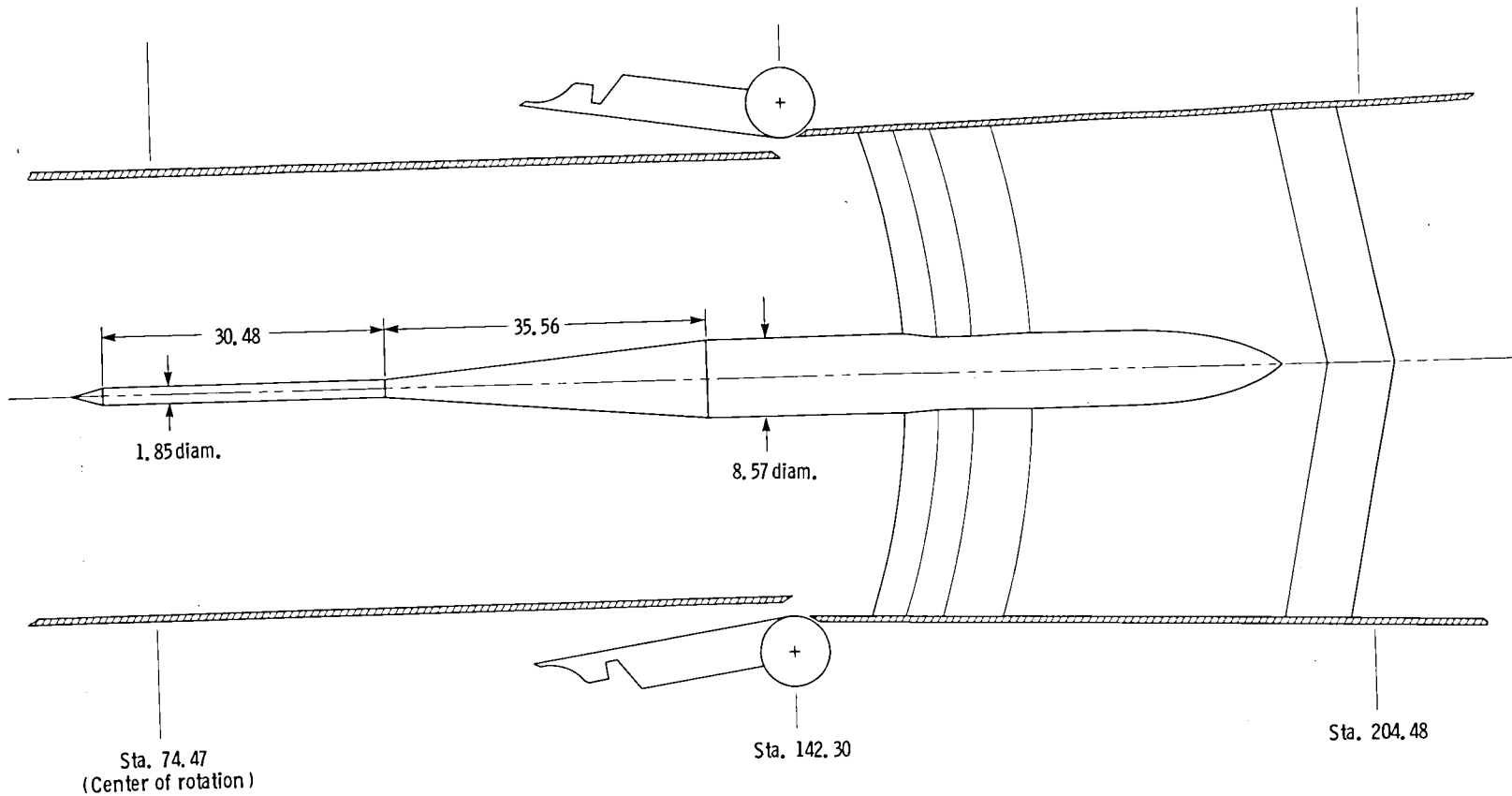
(b) Flaps for vertical wall slots.

Figure 14.- Concluded.



(a) Model support strut.

Figure 15.- Model support strut center body and sting shape for DFA. All dimensions are in centimeters.



(b) Model support center body and sting shape.

Figure 15.- Concluded.

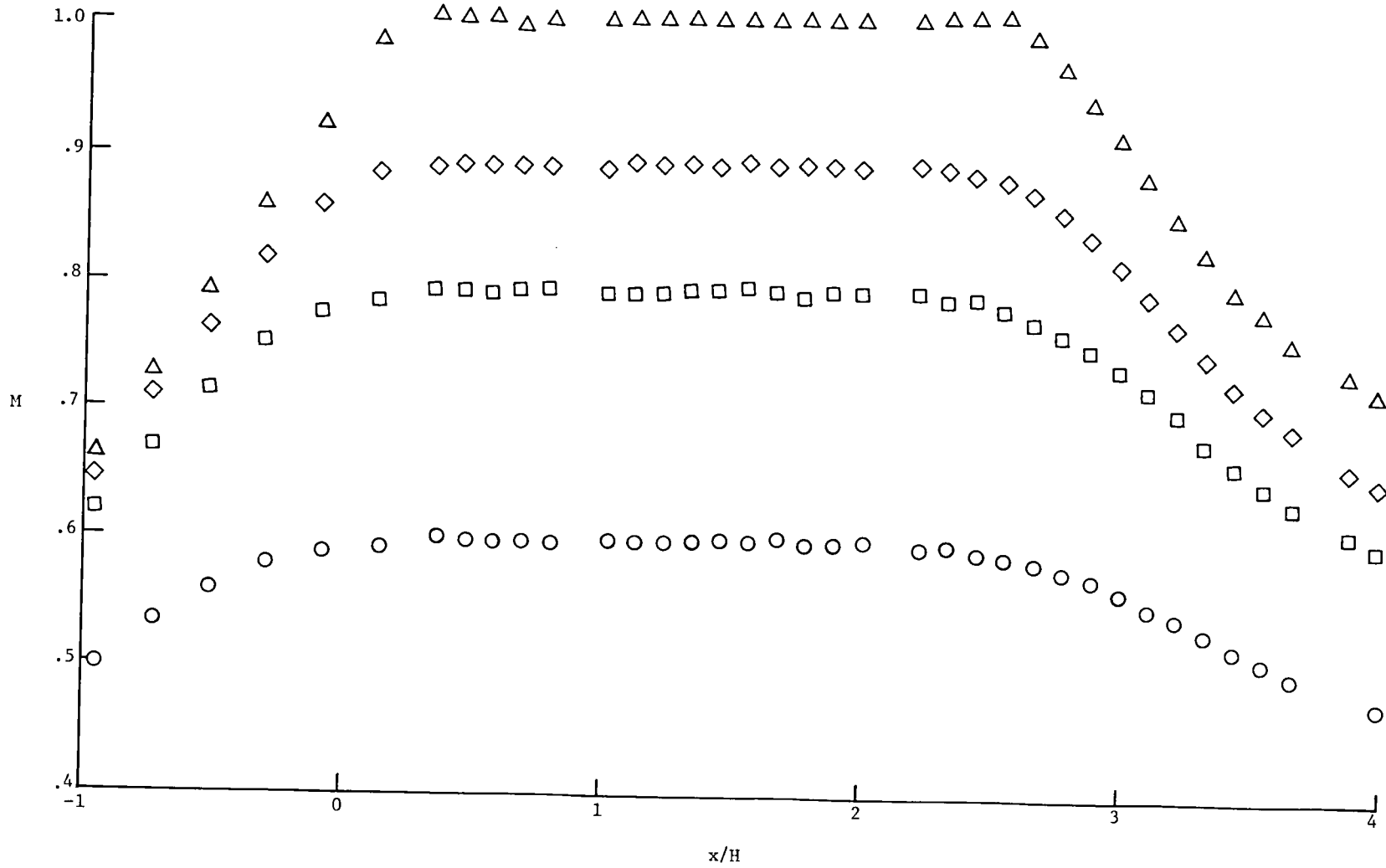


Figure 16.- Mach number distribution along center line of DFA test section with no plenum

suction. $\theta_w = 0.38^\circ$; $\delta_f = -2^\circ$; $\frac{\Delta h}{H/2} = 0.08$.

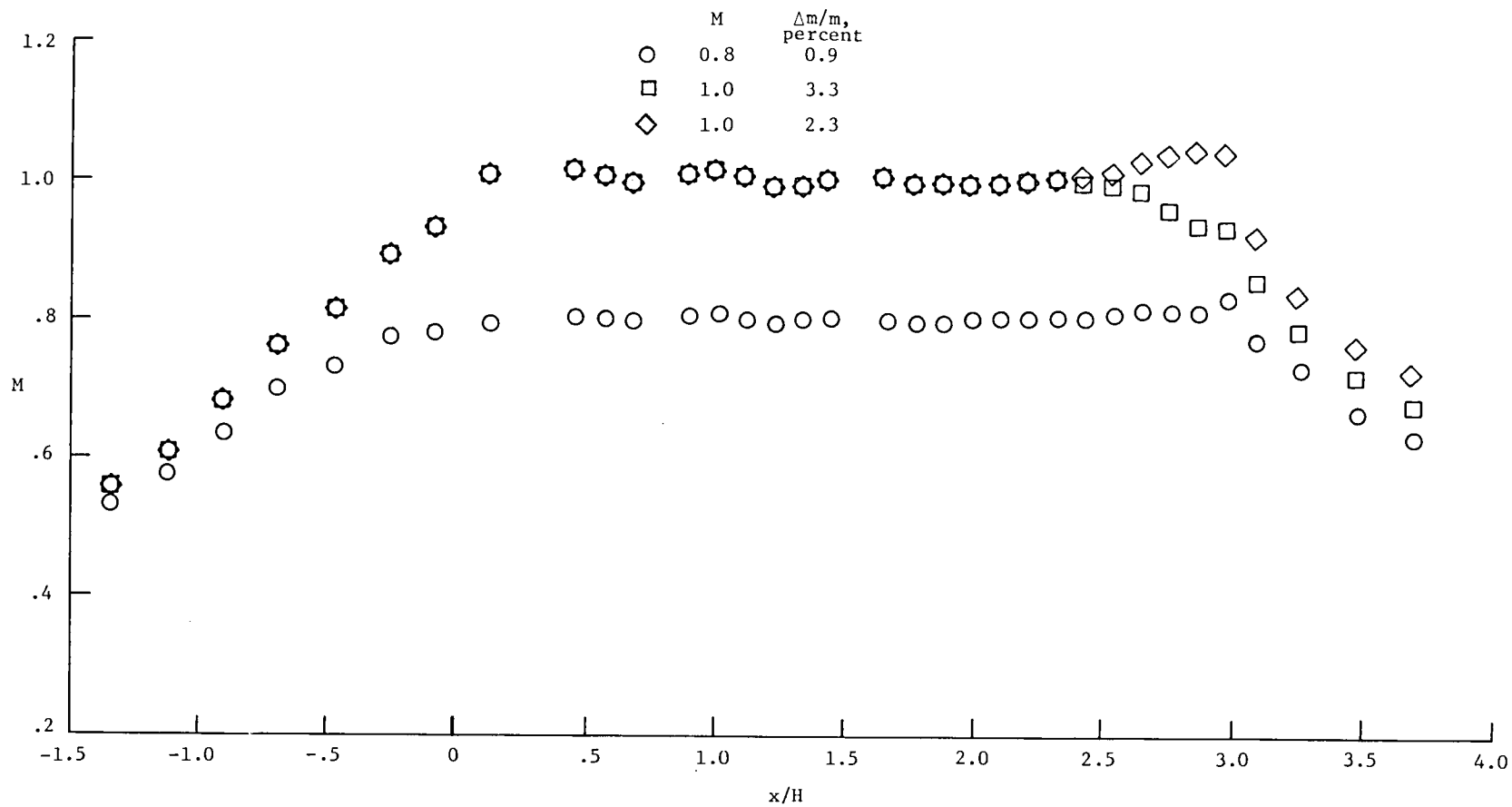


Figure 17.- Effect of plenum suction on wall Mach number distribution in DFA test section.

$$\theta_w = 0^\circ; \quad \delta_f = 0^\circ; \quad \frac{\Delta h}{H/2} = 0.08.$$

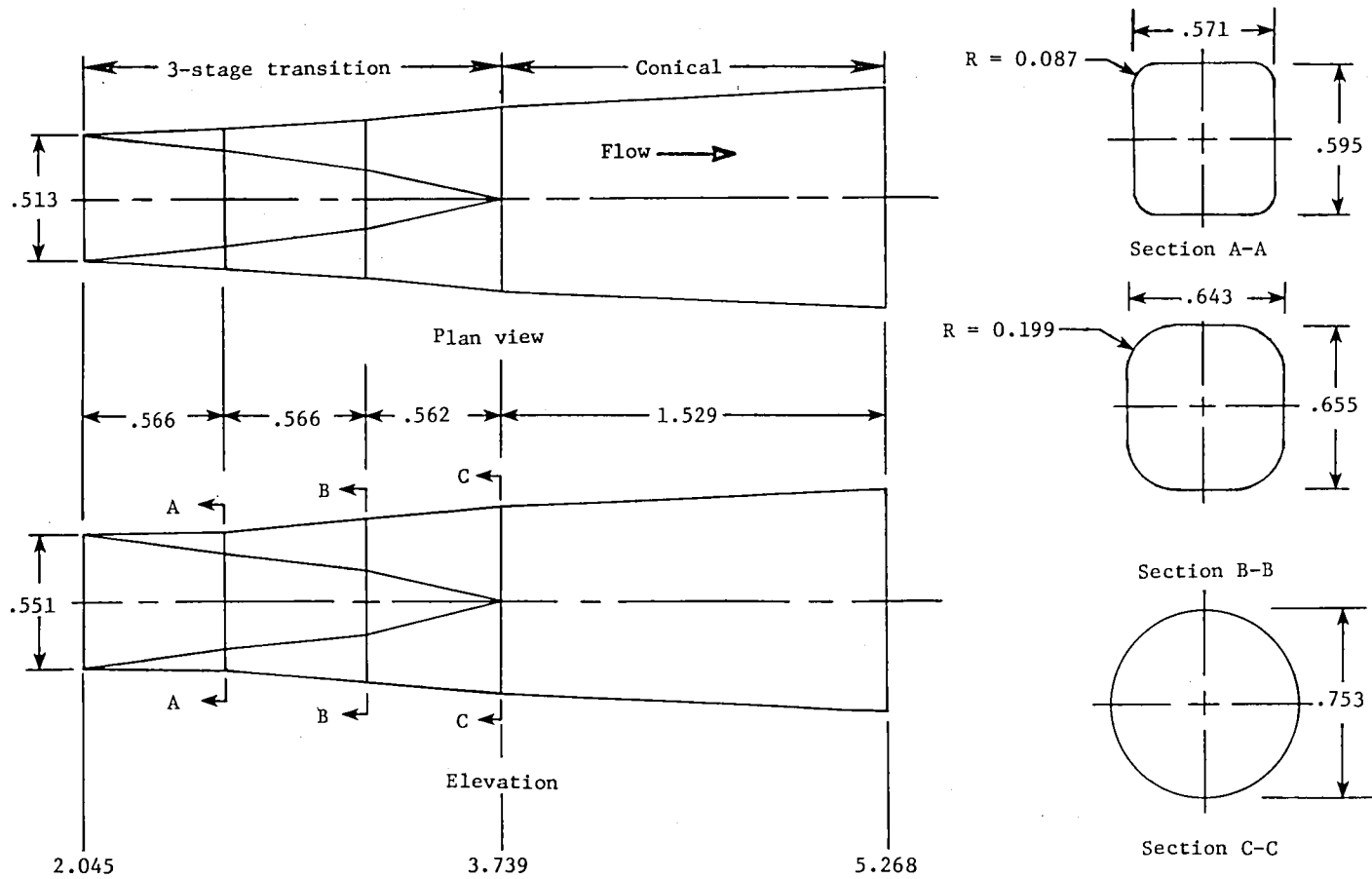


Figure 18.- Geometry of high-speed diffuser for DFA. All dimensions are in meters.

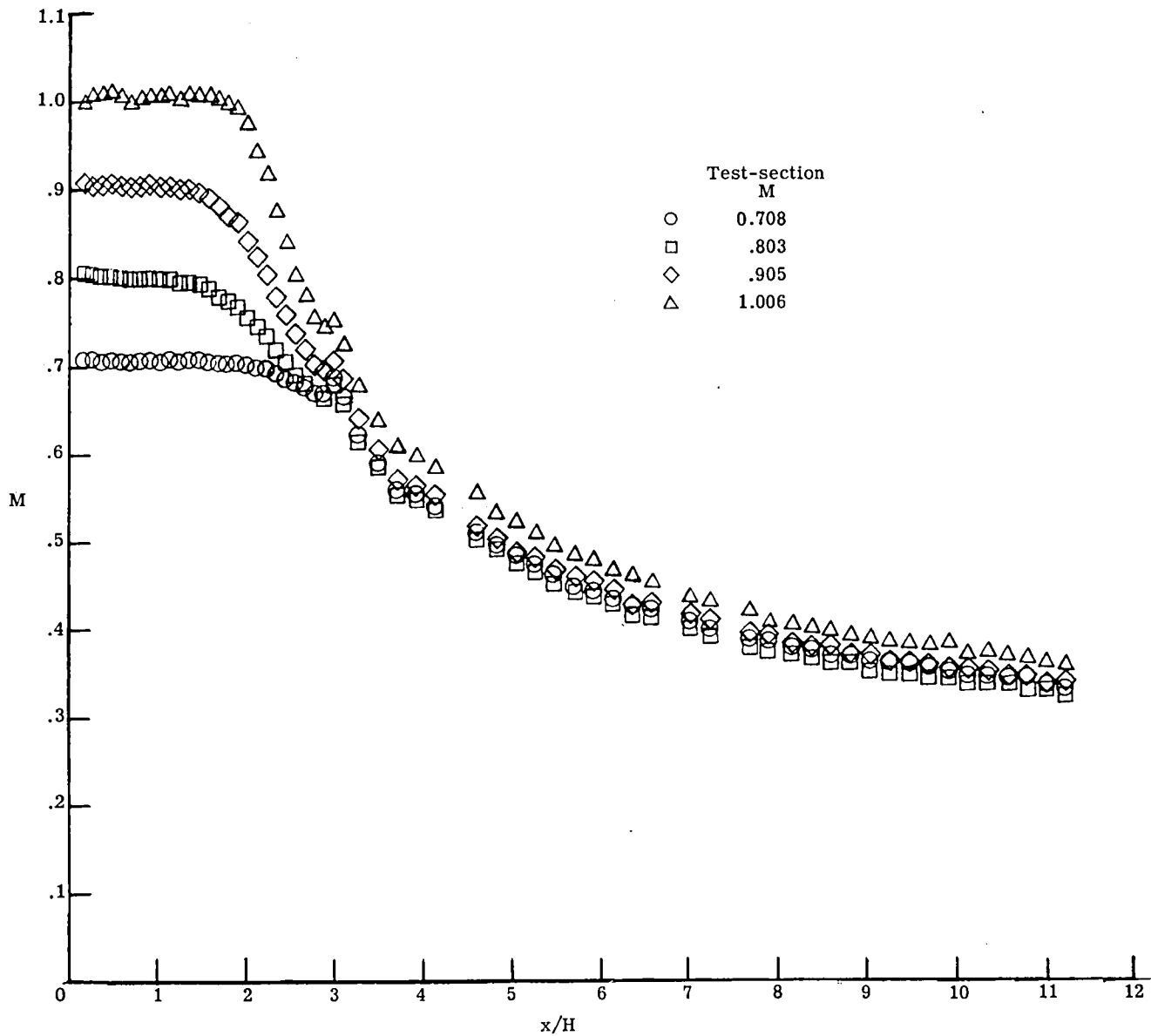


Figure 19.- Longitudinal distribution of Mach number in high-speed diffuser, with plenum suction. $\theta_w = 0.38^\circ$; $\delta_f = -4^\circ$; $\frac{\Delta h}{H/2} = 0.08$.

1. Report No. NASA TM-81949		2. Government Accession No.		3. Recipient's Catalog No.	
4. Title and Subtitle DESCRIPTION OF 0.186-SCALE MODEL OF HIGH-SPEED DUCT OF NATIONAL TRANSONIC FACILITY				5. Report Date May 1981	
				6. Performing Organization Code 505-31-63-01	
7. Author(s) Garl L. Gentry, Jr., William B. Igoe, and Dennis E. Fuller				8. Performing Organization Report No. L-13523	
				10. Work Unit No.	
9. Performing Organization Name and Address NASA Langley Research Center Hampton, VA 23665				11. Contract or Grant No.	
				13. Type of Report and Period Covered Technical Memorandum	
12. Sponsoring Agency Name and Address National Aeronautics and Space Administration Washington, DC 20546				14. Sponsoring Agency Code	
15. Supplementary Notes					
16. Abstract The National Transonic Facility (NTF) is a pressurized cryogenic wind tunnel with a 2.5 m square test section. A 0.186-scale model of the NTF has been used to simulate the aerodynamic performance of the components of the high-speed duct of the NTF. These components consist of a wide-angle diffuser, settling chamber, contraction section, test section, model support section, and high-speed diffuser. The geometry of the model tunnel, referred to as the diffuser flow apparatus (DFA), is described, and some of its operating characteristics are presented.					
17. Key Words (Suggested by Author(s)) Transonic Wind Tunnel National Transonic Facility			18. Distribution Statement Unclassified - Unlimited Subject Category 09		
19. Security Classif. (of this report) Unclassified		20. Security Classif. (of this page) Unclassified		21. No. of Pages 45	22. Price A03



National Aeronautics and
Space Administration

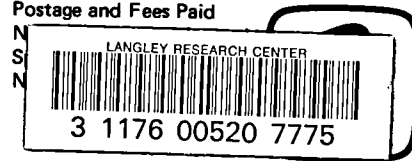
THIRD-CLASS BULK RATE

Postage and Fees Paid

Washington, D.C.
20546

Official Business

Penalty for Private Use, \$300



DO NOT REMOVE SLIP FROM MATERIAL

Delete your name from this slip when returning material to the library.

NAME	MS
Barnes	226
E. Johnson	149
Library	185

NASA Langley (Rev. May 1988) RIAD N-75

If Undeliverable (Section 158
Postal Manual) Do Not Return